hydrology

MDPI

Article

Abandonment Integrity Assessment Regarding Legacy Oil and Gas Wells and the Effects of Associated Stray Gas Leakage on the Adjacent Shallow Aquifer in the Karoo Basin, South Africa

Murendeni Mugivhi [1,*], Thokozani Kanyerere [2], Yongxin Xu [2], Myles T. Moore [3], Keith Hackley [3], Tshifhiwa Mabidi [1] and Lucky Baloyi [4]

[1] Petroleum Agency of South Africa, Heron Place, Heron Cl, Century City, Cape Town 7441, South Africa
[2] Department of Earth Science, University of Western Cape, Bellville 7535, South Africa
[3] Stratum Reservoir (Isotech), LLC., 1308 Parkland Ct., Champaign, IL 61821, USA
[4] Department of Water and Sanitation, Belville Office, 52 Voortrekker Road, Cape Town 7530, South Africa
* Correspondence: mmugivhi@gmail.com; Tel.: +27-726151240

Abstract

Shale gas extraction is underway in the Karoo Basin. Previous oil and gas explorers abandoned several wells, and the abandonment statuses of these wells are unknown. Critically, improperly abandoned wells can provide a pathway for the leakage of stray gas into shallow aquifers and degrade water quality. To understand the abandonment integrity risk posed by these wells, a qualitative risk model was developed to assess the likelihood of well-barrier failure leading to a potential leak. The potential leak paths identified include zones with cement losses during grouting, casing corrosion, cement channels, failure to case and cement risk zones, uncased and uncemented sources, uncemented annuli, and unplugged wells. To confirm whether these wells are leaking, geochemical tracing of stray gas was integrated. Eleven of the fifty samples collected had dissolved hydrocarbon gas concentrations that were high enough to use isotopic analysis to determine the source. The results revealed microbial gas via fermentation and carbon dioxide reduction, thermogenic gas, and geothermal gas, as evidenced by larger $\delta^{13}C_1$ values and isotopic reversals associated with dolerite intrusions. The thermogenic-type gas detected in legacy abandoned wells and <1 km water boreholes adjacent to these wells serves as evidence that the downhole plugs did not maintain their integrity or were improperly plugged, whereas the thermogenic gas detected in >1 km water boreholes indicates leakage contamination due to natural fracture pathways. The presence of thermogenic gas in legacy wells and in groundwater boreholes <1 km from legacy wells implies that shale gas extraction using hydraulic fracturing cannot be supported in these situations. However, using safety buffer zones greater than 1 km from the legacy wells for shale gas drilling could be supported.

Keywords: abandoned wells; barrier failure; isotopic analysis; geothermal gas; Karoo Basin

Check for updates

Academic Editors: Michele Lancia and C. Radu Gogu

Received: 23 October 2025
Revised: 12 December 2025
Accepted: 17 December 2025
Published: 29 December 2025

Copyright: © 2025 by the authors. Licensee MDPI, Basel, Switzerland. This article is an open access article distributed under the terms and conditions of the Creative Commons Attribution (CC BY) license.

1. Introduction

Abandoned wells from legacy oil and gas operations pose a significant threat to shallow aquifers during shale gas extraction. The South African government imposed a moratorium on shale gas extraction in the Karoo following global concerns that the hydraulic fracturing process could contaminate groundwater [1,2]. A landmark concern was reported by Osborn et al. [3] after detecting stray gas in groundwater boreholes near abandoned oil and gas wells situated within 1 km of hydraulic fracturing activities. The

presence of dissolved stray gas in shallow aquifers influences secondary changes in groundwater quality via microbial processes [4–13]. "Stray gas" is defined as gaseous material of undetermined origin found in an area where the gas has impacted the shallow subsurface, potable groundwater supplies, or atmospheric air quality and has the potential to pose a threat to public health and safety [14]. The term includes methane as well as heavier hydrocarbon gases (e.g., ethane, propane, and butane), non-hydrocarbon gases (e.g., nitrogen, carbon dioxide, helium, and oxygen), hydrogen sulfide, and volatile organic compounds (e.g., benzene, toluene, ethylbenzene, and xylenes, collectively called "BTEX") [15].

Dissolved stray gas may also lead to the deterioration of groundwater quality, including borehole water discoloration and turbidity due to microbubbles or particulate suspension [16]. This process occurs through the microbial oxidation of methane gas, reducing iron and sulfate and precipitating sulfide minerals and forming hydrogen sulfide (H_2S) gas. To address such concerns in the Karoo Basin, it is pivotal to identify deep abandoned legacy wells, assess their abandonment integrity, and evaluate whether they are leaking stray gas into proximal shallow aquifers used for household and agricultural activities. Several baseline water quality studies conducted in preparation for shale gas extraction have addressed potential leakage of stray gas in shallow aquifers driven by natural geologic features such as faults and dolerite-induced fractures [17–22] but no studies have examined the abandonment integrity of legacy wells and the potential for stray gas to leak into adjacent shallow aquifers.

Abandoned wells are defined as wells that are unplugged or poorly plugged, have pitted casing, or are poorly cemented at the end of their use [23]. Kang et al. [24] defined abandoned wells as orphaned wells for which the responsible party no longer exists due to bankruptcy. In contrast, Gianoutsos et al. [25] defined abandoned wells as unplugged oil and gas wells that are no longer economically viable but have a responsible owner who is liable for plugging and remediating the well. In this study, we define abandoned wells as wells with either unknown or known locations with either undocumented or documented records that have the potential to leak deep formation fluids into shallower pristine aquifers and the atmosphere. Global records indicate that over a million wells have been abandoned since the start of oil drilling in the 19th century [24,26,27]. Most of these wells have been drilled before the modern regulatory requirements for record-keeping and procedures for well plugging and abandonment at the end of their use. Some of these wells have no surface expression, are in unknown (undocumented) locations [28], and/or were left as gaping holes (or idle) [29].

In the last two decades, the energy industry has boomed following the reinvention of stimulation technology that combines horizontal drilling and hydraulic fracturing, allowing re-entry into old oil and gas fields to unlock previously uneconomic gas resources. These techniques involve the sequential process of drilling, casing, and grouting from vertical to horizontal phases; injecting highly pressurized fluid into the targeted formation; cracking the matrix formation; and creating fissures, thereby increasing the permeability value of the reservoir and enhancing the production of gas [30]. However, researchers have found that applying these techniques in old fields with numerous abandoned wells is environmentally unsafe, as these wells serve as conduits for the migration of subsurface fluid into shallow aquifers, leading to the contamination of groundwater by stray gas [15,31].

This situation has perpetuated a heated debate over whether hydraulic fracturing causes stray gas contamination in shallow aquifers. Researchers have drawn attention to the issue of stray gas contamination due to poor establishment of well integrity during construction and plugging of wells, along with possible long-term cement deterioration after abandonment [27,32–35]. Others argue that stray gas (mainly methane) in shallow aquifers occurs naturally. Such gas is common in aquifers underlain by hydrocarbon-rich

formations, and the resulting contamination is not linked to abandoned wells but instead driven by natural fractures, particularly in structurally complex areas [15,20,36,37].

To address this controversy in the context of a typical frontier basin like the Karoo, a detailed investigation of abandoned legacy wells—focusing on assessing construction and plugging integrity status and determining the extent to which stray gas has leaked into water boreholes adjacent to the wells—is essential. This work will help determine whether legacy well operations affected shallow aquifers. An integrated approach combining well barrier failure assessment and geochemical tracing can foster a comprehensive understanding of deep wells in Karoo and their potential impacts on shallow aquifer systems. Reconstruction of well schematics from well data recorded in completion reports can serve as an integrity assessment tool for evaluating well barrier failure and identifying leak paths in abandoned wells [38]. Geochemical tracing involving hydrocarbon dissolved gas concentrations and isotopic characterization provides information that can be used to determine whether stray gas in shallow groundwater systems originated from methanogenesis or thermogenic processes [31].

This study focuses on fifteen abandoned well-sites within 160,000 square kilometers of the Karoo region targeted for shale gas extraction. First, we assessed the integrity of abandoned wells, evaluated potential leaks using four wells with well completion reports, and extrapolated the results to the remaining 11 wells without completion reports. Then, we collected groundwater samples to determine dissolved gas concentrations and conducted isotopic analyses of stable carbon and hydrogen ($\delta^{13}C$ and δD) in methane (CH_4) and of $\delta^{13}C$ in ethane and propane to characterize gas sources. This integrated analysis provides findings on improperly abandoned Karoo wells and their potential to leak stray gas into adjacent shallow aquifers. Thus, this study provides scientific evidence that can be used to either support or refute shale gas exploitation. The outcome of this study informed the development of decommissioning guidelines (Petroleum Agency SA internal report) for onshore wells to prevent continued well leakage after well decommissioning and abandonment. This evidence will also help the national government make informed decisions on the upliftment of the moratorium.

2. Description of the Study Area

2.1. Study Area

The study area is in a region targeted for shale gas exploration by Shell, Bundu Gas & Oil, and Falcon Oil & Gas before the moratorium (Figure 1). The area contains 14 legacy wells drilled by Soekor (Pty) Ltd. in search of commercial oil reservoirs and 1 Karoo Deep Drilling (KDD) well drilled by the Council for Geoscience (CGS) to investigate shale gas potential. We did not sample all 15 wells (14 legacy wells and the CGS well) in this study. The wells and the towns in which they were drilled include B390/1 (in Ceres), SA 1/66 (in Merweville), KDD (in Beaufort West), KW 1/65 (in Prince Albert), VR 1/66 (in Graaff-Reinet), CR 1/68 (in Pearston), SC 3/67 (in Aberdeen), KA 1/65 (in Murraysburg), AB 1/65 (in Victoria West), KD 1/71 (in Carnarvon), KC 1/71 (in Calvinia), AM 1/70 (in Williston), Qu2/65 and Qu1/65 (in Fraserburg), and KL 1/65 (in Sunderlands). These wells were drilled before modern regulations, such as Oil and Gas UK [39] and NORSOK D-010 [40], were introduced to prescribe how wells must be treated before decommissioning and abandonment.

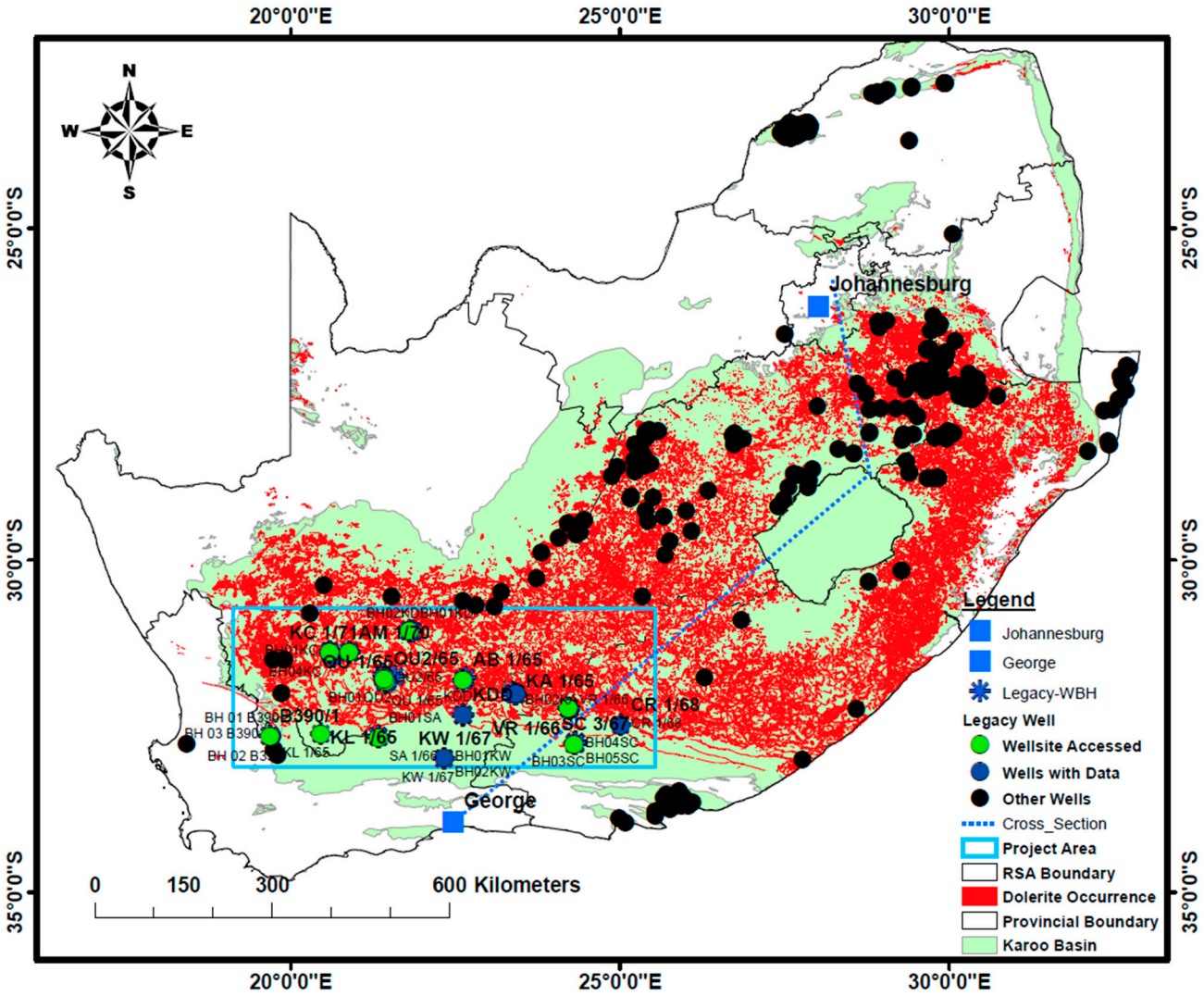


Figure 1. Map of the project area showing Karoo's geology, deep well locations, and the groundwater boreholes selected.

For a few of the wells (CR 1/68, KW 1/67, KA 1/65, and KDD), there are records on how they were constructed and abandoned, whereas for others (B390/1, SA 1/66, KW 1/65, VR 1/66, CR 1/68, SC 3/67, AB 1/65, KD 1/71, KC 1/71, AM1/70, Qu2/65, Qu1/65, and KL 1/65), there are no records. Site visits in the project area revealed that some of the wells have surface expressions (KDD, KW 1/65, KA 1/65, VR 1/66, AM1/70, and KL 1/65), whereas other wells had casings cut below the ground (B390/1, CR 1/68, KD 1/71, KC 1/71, and Qu2/65). To conduct groundwater sampling for dissolved stray gas and isotopic analysis, we relied on existing boreholes drilled by the farmers for household and agricultural activities. The boreholes were selected based on their proximity to the legacy well site and are denoted by "BH" at the front of the name (Table 1). The legacy wells in the study area (KDD, KA 1/65, Qu1/65, and KL 1/65) intersect the Ecca group shales, a thermally mature hydrocarbon gas bearing group, with the potential to leak through these legacy wells into shallow aquifer systems. To investigate potential leakage from legacy wells into shallow aquifers, the boreholes shown in Figure 1 (blue and green dots) and listed in Table 1 were selected for this study. Due to farm owners denying access, some of the shallow boreholes surrounding the legacy wells could not be sampled.

Table 1. Legacy wells and surrounding groundwater boreholes selected for the study. The peach shading denotes the deep wells.

Legacy Wells	Boreholes	Farm	Town	Borehole Depth (mbgl)	Proximity to Deep Well
B390/1	BH 01 B390/1	Blaauwbosch Kalk	Ceres	100.0	0.5 km
	BH 02 B390/1	Blaauwbosch Kalk	Ceres	132.2	1.2 km
	BH 03 B390/1	Blaauwbosch Kalk	Ceres	83.5	1.3 km
SA 1/66	BH 01 SA	Sambokraal	Merweville	85.0	1.0 km
	BH 02 SA	Sambokraal	Merweville	50.0	2.0 km
	BH 03 SA	Sambokraal	Merweville	73.4	3.0 km
KDD	KDD	Commonage Land	Beaufort West	2978	0
	B 02 H–BW KDD	Commonage Land	Beaufort West	169.0	0.5 km
	B 04 H–BW KDD	Commonage Land	Beaufort West	169.0	1.0 km
	SPF-BW KDD	Commonage Land	Beaufort West	144.5	1.5 km
KW 1/67	BH 01 KW	Klein Waterval	Prince Albert	24.0	0.1 km
	BH 02 KW	Klein Waterval	Prince Albert	34.0	0.2 km
VR 1/66	BH 01 VR	Vrede	Graaff-Reinet	10.0	0.4 km
	BH 02 VR	Vrede	Graaff-Reinet	12.0	0.75 km
	BH 03 VR	Vrede	Graaff-Reinet	12.0	1.0 km
	BH 04 VR	Vrede	Graaff-Reinet	23.0	3.0 km
SC 3/67	BH 01 SC	Skietfontein	Aberdeen	50.0	0.75 km
	BH 02 SC	Skietfontein	Aberdeen	50.0	1.5 km
	BH 03 SC	Skietfontein	Aberdeen	50.0	4.0 km
	BH 04 SC	Skietfontein	Aberdeen	50.0	1.75 km
	BH 05 SC	Skietfontein	Aberdeen	50.0	1.0 km
KA 1/65	KA 1/65	Karee Bosch	Murraysburg	2600.0	0
	BH 01 KA	Karee Bosch	Murraysburg	100.0	6.5 km
	BH 02 KA	Karee Bosch	Murraysburg	50.0	2.0 km
	BH 03 KA	Karee Bosch	Murraysburg	25.0	3.0 km
AB 1/65	BH 01 AB	Abrahamskraal	Victoria West	65.0	1.5 km
	BH 02 AB	Abrahamskraal	Victoria West	85.0	3.75 km
KD 1/71	BH 01 KD	Heuwels	Carnarvon	132.0	0.25 km
	BH 02 KD	Heuwels	Carnarvon	100.0	1.5 km
	BH 03 KD	Heuwels	Carnarvon	78.0	4.0 km
	BH 04 KD	Heuwels	Carnarvon	55.0	6.0 km
KC 1/71	BH 01 KC	Kwaggasfontein	Calvinia	72.0	0.75 km
	BH 02 KC	Kwaggasfontein	Calvinia	60.0	1.0 km
	BH 03 KC	Kwaggasfontein	Calvinia	55.0	9.0 km
	BH 04 KC	Kwaggasfontein	Calvinia	45.0	10.5 km
AM 1/70	BH 01 AM	Amersfontein	Williston	25.0	0.6 km
	BH 02 AM	Amersfontein	Williston	25.0	0.75 km
	BH 03 AM	Amersfontein	Williston	20.0	1.8 km
	BH 04 AM	Amersfontein	Williston	22.0	1.0 km
CR 1/68	Not sampled due land access issues				

Table 1. *Cont.*

Legacy Wells	Boreholes	Farm	Town	Borehole Depth (mbgl)	Proximity to Deep Well
QU 2/65	BH 01 QU2	Beeswater	Fraserburg	53.0	1.0 km
	BH 02 QU2	Beeswater	Fraserburg	60.9	500 m
	BH 03 QU2	Beeswater	Fraserburg	74.4	200 m
	BH 04 QU2	Beeswater	Fraserburg	95.0	16.0 km
	BH 05 QU2	Beeswater	Fraserburg	25.0	8.0 km
QU 1/65	QU1/65	Quaggasfontein	Fraserburg	2490.0	0
	BH 01 QU1	Quaggasfontein	Fraserburg	70.0	1.5 km
	BH 02 QU1	Quaggasfontein	Fraserburg	35.0	2.0 km
	BH 03 QU1	Quaggasfontein	Fraserburg	5.0	1.8 km
	BH 04 QU1	Quaggasfontein	Fraserburg	30.0	1.9 km
KL 1/65	KL 1/65	Klipdrift	Sutherlands	3500.0	0

Peach shading denotes deep wells sampled.

2.2. Geological Setting

The Karoo Supergroup basin was deposited during the early Carboniferous to middle-Jurassic periods (Figures 2 and 3) [41]. The basin is underlain by the Kaapvaal Craton to the north and the Cape Supergroup to the South. It has resulted from episodic tectonic extension and compression that contributed to the development of Southern Gondwana beginning in the Late Precambrian (Figure 3). During the Late Paleozoic era, the southern margin of Gondwana transformed into an Andean-style foreland Basin or intracratonic Basin, thus forming the Karoo Basin [42]. This basin succeeded the Late Proterozoic to early Paleozoic Cape supergroup that forms the basement in the south [43].

The Karoo Basin developed synchronously with the subduction of the paleo-Pacific Plate beneath the Panthalassan margin of Gondwana. The Gondwanide Magmatic Arc—a series of fold–thrust belts, including the Cape Fold Belt—and a sedimentary basin system, including the Karoo Basin, formed in association with this subduction zone. The Cape Fold Belt, which bounds the southern Karoo basin to the west and south, formed from deformation of Paleozoic metasedimentary and sedimentary rocks during the Permian–Triassic Cape Orogeny [44]. Later Mesozoic rifting of Gondwana resulted in the formation of a passive margin along southern Africa, and remnants of the Gondwanide convergent margin system were preserved in South America, Africa, the Falkland Islands, Antarctica, and Australia [45].

Woodford and Chevallier [46] also suggested that the development of the Karoo Basin was controlled by four major geodynamic events, during which the Karoo Supergroup was deposited in a foreland basin during the formation of the Cape Fold Belt (~250 Ma). Karoo sediment deposition was terminated by the onset of the Gondwana break-up that occurred alongside the intrusion of the Jurassic dolerite and the extrusion of the Drakensberg flood basalts (~180 Ma), intra-plate mantle activities emplacing kimberlite pipes, and fissures accompanied by intrusion of carbonate plugs and epeirogenic uplift with enhanced erosion rates during the formation of the Kalahari plateau (~140 to 80 Ma), followed by declining rates of erosion and the establishment of modern river systems (~60 Ma to the present). The first depositional event consisted of glacial deposits that formed the Dwyka Group, with the first sediments to be deposited in the developing Karoo depression. This group is thickest in the South along the Cape Mountain front. In the northern part of the Basin, where water was shallow, the glacial ice was grounded along an elevated region that extends to the Cargonian highlands. Seasonal melting of the glacial ice left behind vast quantities of mud and large rock fragments, which formed the poorly sorted Dwyka formation, consisting of

tillite, diamictite, conglomerate, immature sandstone, and varved mudstone [47]. These deposits are very thin or non-existent on the Cargonian highlands, which form the northern edge of the Karoo inland sea.

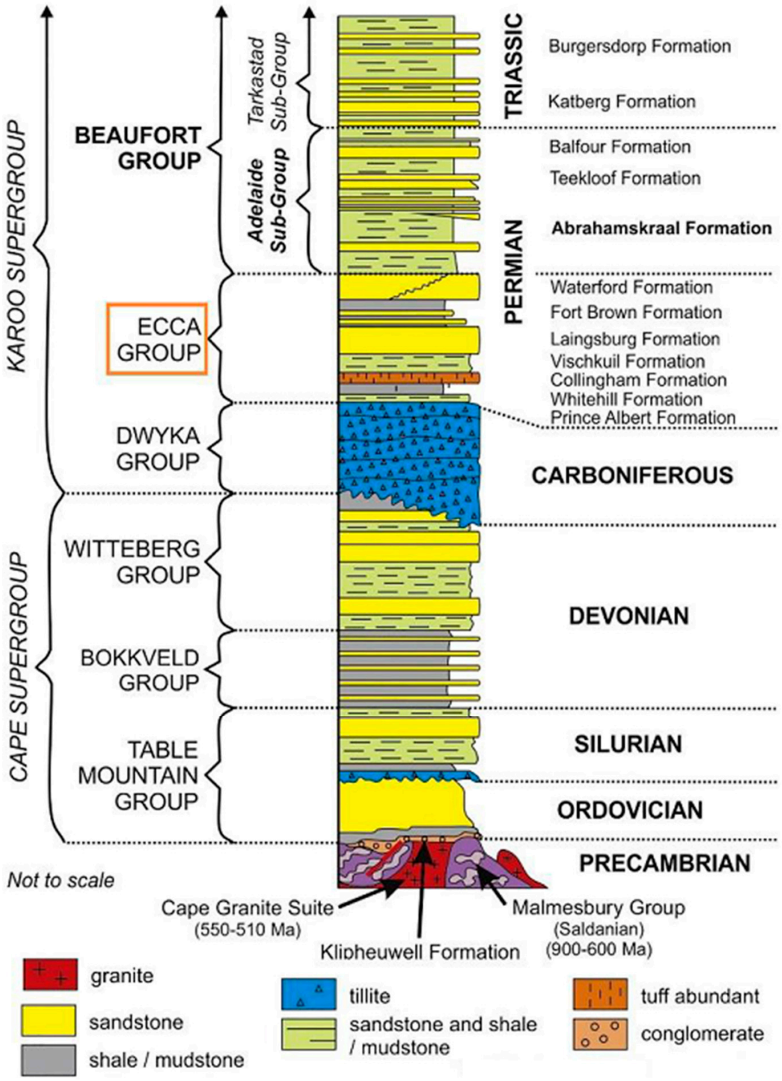
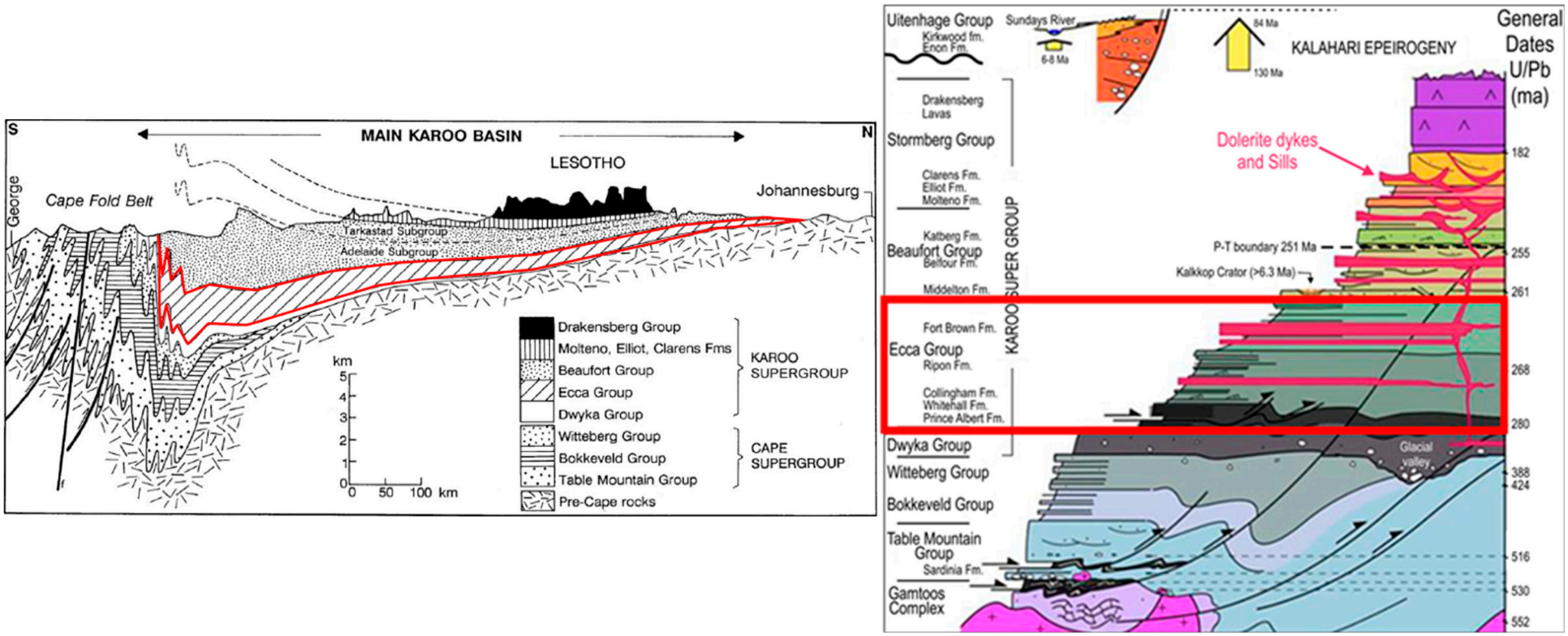


Figure 2. Simplified stratigraphic column of the southern Karoo Basin, with a peach box denoting the Ecca Group formation of the Karoo Supergroup, targeted for shale gas extraction [41].

The second group deposited in the Karoo Basin is the Ecca Group (highlighted in Figure 3), which formed during further environmental fluctuations as Gondwana continued to drift, resulting in deep-sea deposits of sandstones and mudrocks. The deposition of these sediments revealed an anoxic, suboxic-to-oxic environmental condition with high concentrations of organic material, indicating a shift from low- to high-energy deposition [48]. Depositions of these organic-rich strata were potential targets for the past drilling campaign in search of commercial oil reservoirs [49] and are currently potential targets for shale gas exploitation [50]. The targeted organic-rich shales in this group are the Prince Albert, Collingham, Whitehill, and Tierberg formations. Assessment of unconventional hydrocarbon potential revealed that the total organic carbon (TOC) content of the Prince Albert formation's shales varies by up to 12 wt.%, with the Whitehill shales ranging up to 15 wt.% and the Tierberg shales averaging 1–2 wt.% [51]. This observation encouraged industry developers to re-examine the Karoo Basin and show interest in exploiting shale gas through horizontal drilling and hydraulic fracturing.



(**a**) (**b**)

Figure 3. Generalized cross-section of the geology of the Karoo Basin from the south/southwestern part of the basin to the northeastern part of the basin in South Africa (**a**), reproduced from [46]. (**a**) shows the geology along the blue dashed line from George to Johannesburg in Figure 1. Also shown is a stratigraphic column of the Karoo Basin (**b**), reproduced from [47,48]. It is essential to note the dolerite dykes and sills (denoted in pink) that intrude throughout the Karoo Supergroup (see Figure 1). The Ecca Group, which contains organic-rich shales, is outlined in red in the diagrams above.

The preservation of the succeeding Beaufort Group sediments above the Ecca Group reveals the depositional transition from marine to fluvial systems, resulting in interbedded sandstone and mudrock. The aeolian-deposited sandstone and shale of the Stormberg Group overlie this group. The end of the Karoo sedimentation was marked by the initial fragmentation of Gondwana, an event that introduced the Drakensberg flood basalts and dolerite intrusions (Figure 3b) [52]. These volcanic intrusions are considered significant events associated with the break-up of the Gondwana supercontinent and the formation of the South Atlantic [53], which also affected other southwest Gondwanan Basins, including the Parana Basin in Brazil, e.g., [54]. Dolerite intrusions have cut across the entire Karoo sequence [46], with the thickest sills located within the Ecca Group. These dolerite intrusions triggered metamorphism of the organic-rich shales as they cut through them, releasing gas from the shale formations (Figure 3b) [55].

Regarding shale gas exploitation, the Ecca group is the main target and requires careful evaluation of this resource in the respective targeted formation (Figure 3, highlighted in red). Smithard et al. [56] recommended that assessments of unconventional resources in this group should consider subsurface thickness and the spacing of volcanic intrusive bodies within the targeted formations. This recommendation was brought forward following the observation that dolerite intrusions in this group have metamorphosed, hosting shale gas formations. The risk posed by these intrusive features was also noted by Nengovhela et al. [52], who reported that these features have expelled natural gas from the host rock into the atmosphere and shallow aquifers. Despite the consequences of the volcanic intrusions possibly expelling large volumes of natural gas, these intrusions have facilitated the host rock's maturation, thereby increasing the amount of natural gas within it [51]. The influence of dolerite intrusions with temperatures reaching 600 °C and the hydrothermal fluids generated [52] are expected to affect the isotopic signature of the natural gas formed. Typically, hydrocarbon generation is expected to follow a normal trend in regard to alkane isotopes, with methane having the most negative $\delta^{13}C$ value, followed by ethane and then propane ($\delta^{13}C_1 < \delta^{13}C_2 < \delta^{13}C_3$). In a situation where dolerite intrusion and hydrothermal fluids have influenced hydrocarbon generation, a reversal of this normal trend in alkane $\delta^{13}C$ values could occur ($\delta^{13}C_1 > \delta^{13}C_2$ and/or $\delta^{13}C_2 > \delta^{13}C_3$) [57–59]. This study's geochemical analyses also account for the influence of dolerite intrusion and hydrothermal fluids on the isotopic signatures of the generated hydrocarbon alkanes.

2.3. Hydrological Conditions

The Karoo Basin aquifers are hosted in the Dwyka, Ecca, and Beaufort groups with a Jurassic-age dolerite intrusion providing a target for borehole siting [53]. Drinking water boreholes are drilled shallower than 200 m (m) deep and typically have water table depths of 5 to 15 m [60]. Recharge occurs during seasonal flooding, primarily through fractured rock aquifers and dolerite-related fractures [61]. The hosting and producing groundwater lithologies vary by locality. In the Dwyka group, the diamictite and shale have very low hydraulic conductivities (~10^{-11} to 10^{-12} m/second), yielding low flows associated with narrow joints and fractures [46]. Groundwater in these lithologies was found to be brackish, with total dissolved solids (TDS) ranging from 1390 to 10,010 mg/L [60]. The Ecca group is dominated by shale and mudstone lithologies with no major aquifer systems. Borehole tests yielded >5 L/second of flow, particularly where intrusive structures intersect bedding-plane fractures [46]. In the Beaufort group, groundwater is produced primarily by fractured rocks of the Adelaide Subgroup, the Tarkastad Subgroup, and the Molteno, Elliot, and Clarens Formations, as well as from shallower fluvial deposits [62]. Aquifers in this group are multi-layered and heterogeneous, with the highest yields witnessed in contact zones between host formation and intrusive structures [46].

Groundwater also occurs in geothermal springs linked to deep fractures such as dolerites [22]. Hohne et al. [17] reported that dolerite ring structures release methane gas and are understood to connect deeper Ecca Group shale formations with shallower Beaufort Group aquifers (Figure 3b). This connection suggests that possible mixing of deeper and shallower waters is driven by recurring micro seismicity in the vicinity. The seismic events are also linked to groundwater boreholes turning artesian. Senger et al. [63] found that conduit structures within dolerite intrusions also serve as pathways for subsurface fluids, including brine, hydrocarbons (CH_4, C_2H_6, and C_3H_8), and non-hydrocarbon gases (CO_2 and H_2S), with the potential to degrade groundwater quality. Regions farther from the legacy wells may be affected by stray gas not linked to the legacy wells' operations, but rather through natural fractures. Although groundwater recharge is associated with fractured lithologies, including fractured dolerites, the preferential regional-scale flow is topographically controlled and trends in different directions across the study area. In the western part (in the towns of Calvinia and Williston), the direction of flow in shallow aquifers is northward. In the central part (Fraserburg and Beaufort West), the flow path trends from the north to southwest, south, and southeast. In the eastern part (Murraysburg, Graaff-Reinet, and Aberdeen), the flow path runs to the east [60]. These directional flow paths are also directional paths for dissolved stray gas in the aquifer system. Most groundwater studies were based on deep geological investigations of Karoo legacy wells [46,53,60,62]. These wells enhance our understanding of the deeper geological and hydrological setting of the Karoo Basin, as noted by Talma and Esterhuyse [22], Harkness et al. [19], and Eymold et al. [20].

3. Advocacy for Well Integrity Based on Modern Industry Practices and Regulations

Modern industry practices [64] and statutory regulations [39,40] were introduced to promote the adoption of zero-leak acceptance criteria for oil and gas wells. These practices and guidelines were reviewed to qualify and demonstrate the use of a well barrier assessment to evaluate the abandonment integrity of Karoo deep wells. This review focused on synthesizing industry practices and regulatory guidelines to establish a strategy for evaluating the well barrier elements (WBEs) of abandoned wells. According to these industry practices and regulations, all wells in operation must secure well integrity through WBEs, including primary and secondary well barriers, to effectively isolate formations with flow potential during drilling, well testing, well completion, well production, well suspension (temporary abandonment), and permanent abandonment. The primary well barrier is the first barrier that prevents flow from a potential inflow source, and the secondary well barrier is the second barrier that prevents flow from a potential inflow source. The second barrier is meant to isolate the well if the primary barrier fails. At each stage, whether that is drilling, testing, completion, production, temporary abandonment, or permanent abandonment, these WBEs are tested for effective sealing.

During drilling, the first WBE is the drilling fluid, which is circulated downhole through the drill string and up the space between the drill string and wellbore. Drilling fluid serves to lubricate the drilling assembly, remove formation cuttings, maintain well pressure control, and stabilize the hole being drilled. This fluid is typically a mixture of water, clays, fluid-loss control additives, density-control additives, and viscosifiers. Drilling fluid is a carefully monitored and controlled mixture designed to achieve the best drilling results. The first section of the hole to be drilled is the conductor phase, in which conductor casing is installed (Figure 4A,A'). The conductor casing can also be driven into place, like a structural piling, in some circumstances. This phase is followed by the drilling of sequentially deeper holes to install the surface casing (Figure 4B,B'), intermediate casing

(Figure 4C,C′) (if necessary), and production casing (Figure 4D,D′). Casings are the second set of WBEs installed to secure and maintain well integrity. Crucially, a well is drilled in telescoping-down phases to manage wellbore stability and install monitoring equipment to ensure adequate well integrity. After casing installation, the subsequent phase consists of placing cement grouting between the rock and the casing to achieve zonal isolation and ensure integrity. Good isolation requires complete annular filling and tight cement interfaces with respect to the formation and casing. Complete displacement of the drilling fluid by cement and good bonding of the cement interfaces between the drilled hole and the casing immediately above the hydrocarbon formation are key components of well and seal integrity. After each cement grouting phase, the hole is pressure-tested using a leak-on test (LOT) to ensure there is no potential leakage during subsequent drilling.

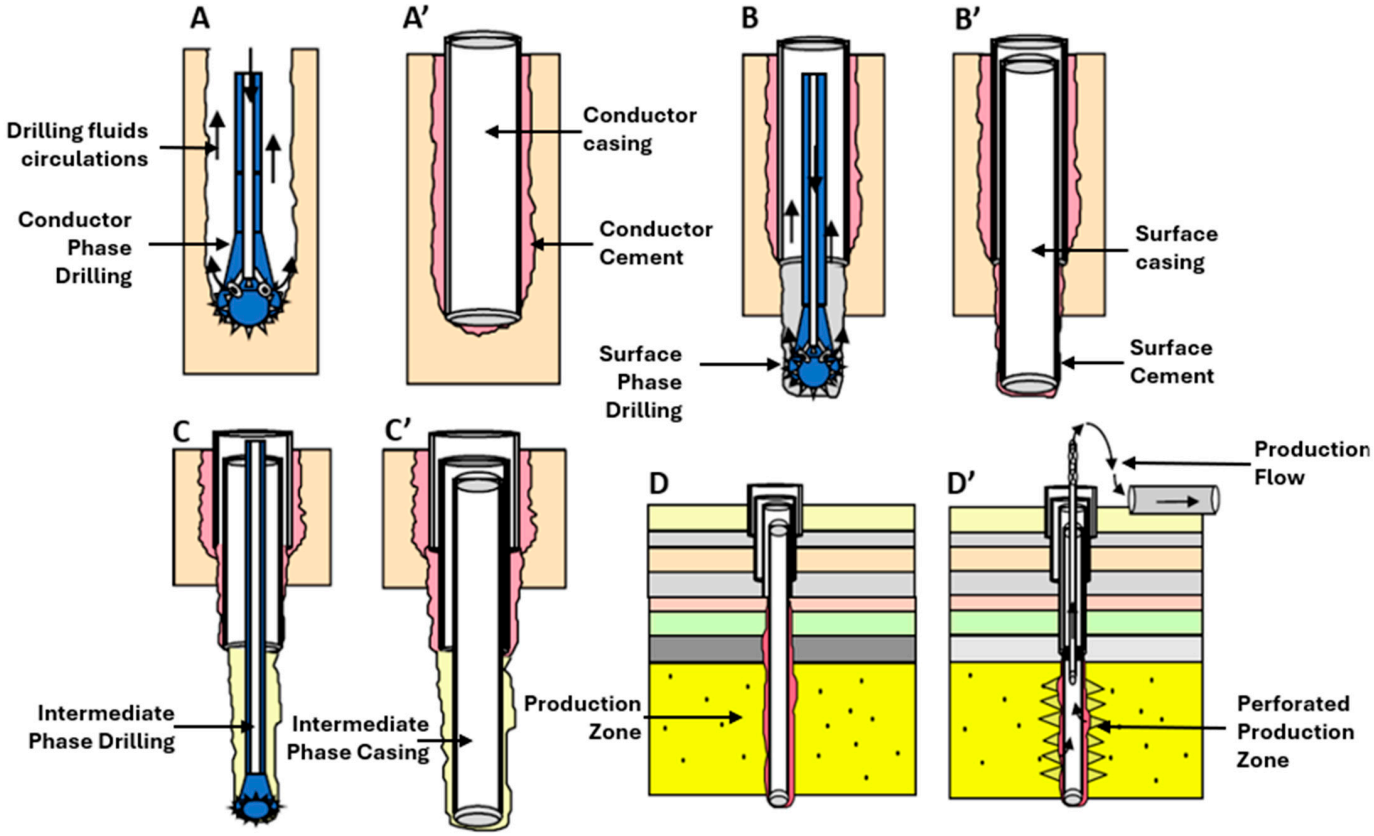


Figure 4. Schematic diagram illustrating cyclic drilling, casing, and cementation of a well telescoping down into geological formations in phases—(**A**) conductor, (**B**) surface, (**C**) intermediate, and (**D**) production—to maintain well integrity. (**A**–**D**) further demonstrate the capacity of drilling fluids to maintain well integrity during drilling, and (**D**) also demonstrates their capacity during well perforation and production.

The integrity of cement placement is further qualified using a cement bond log (CBL). This log measures the presence of cement and the quality of the cement bond or seal between the casing and the formation. This information is acquired using an acoustic device that can detect whether the casing is cemented or non-cemented. This device transmits sound or vibration signals and then records the amplitude of the arrival signal. A casing with no cement surrounding it (a free pipe) will produce a large-amplitude acoustic signal because the energy remains in the pipe. On the other hand, casing that has a good cement sheath that fills the annular space between the casing and the formation will have a much smaller amplitude signal since the casing is "acoustically coupled" with the cement and the formation, causing the acoustic energy to be absorbed. This coupling is the main

feature that creates the desired isolation. The variable density log (VDL) is a commonly shown display with the CBL and shows the wave train of an acoustic signal. Monitoring equipment, such as blowout preventers (BOPs), constitute another WBE for controlling the well. These practices and regulations also dictate the requirements for permanent plugging and abandonment when wells reach the end-of-life stage; the last WBE in the well that prevents fluids from crossing over to the successive formations. Before plugging, a well history record must be reviewed and assessed to ensure that all WBEs in place during construction, completion, and production are effective and that no leaks have occurred. This also includes creating a well barrier schematic (WBS) to determine the status of a well upon completion; demonstrating all the sources of inflow identified; determining the depths of casing strings and cement and specifying the types used; documenting intersected stratigraphy; creating logs for cement bond verification; determining well condition, including with respect to scale build-up, casing wear, collapsed casings, H_2S, CO_2, hydrates, and benzene; and specifying the number and depths of barriers to be placed. Zones with potential flow must be permanently plugged with two potential plug barriers at the designated depth (Figure 5).

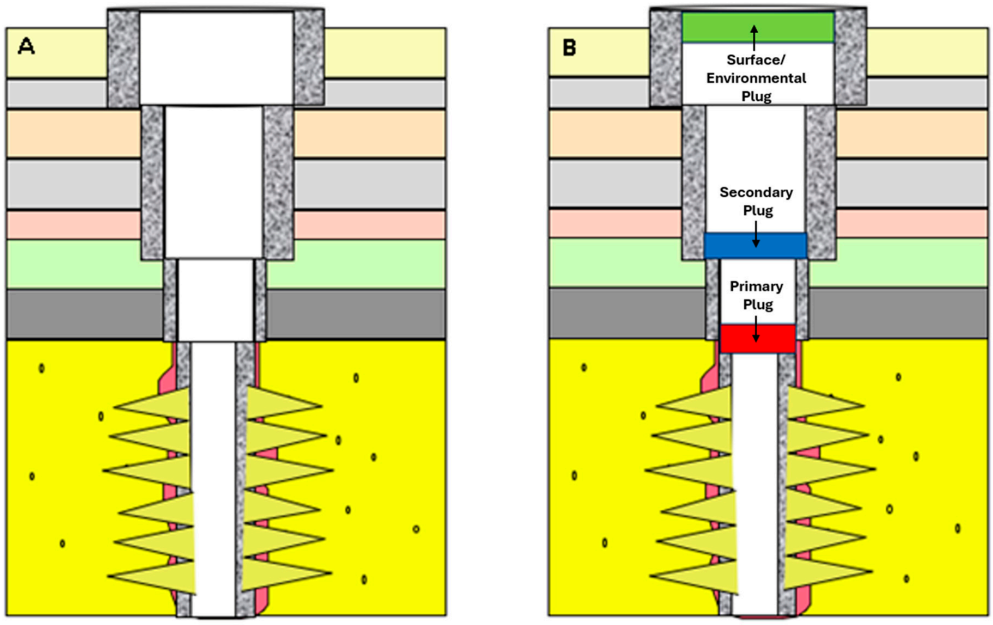


Figure 5. Schematic diagram of a well drilled into the yellow target formation at the end of use: (**A**) upon removal of equipment, and (**B**) in-place plugs (red—primary plug barrier, blue—secondary plug barrier, and green—surface environmental plug) used to plug the well permanently.

Primary and secondary barriers may be combined into a single large permanent barrier, provided it is effective and reliable in achieving the objective. The length of the barrier varies from 30 to 100 m, depending on the regulator's requirements and the geological zone to be sealed. Upon completion, the barrier must be tested and verified to ensure effective sealing. The method for verifying sealing capacity is either tagging or measuring to confirm the depth of the firm cement plug. In an open hole, a barrier should be verified by conducting a weight test on a drill pipe, applying 10 to 15 klbs, or by using a wireline with coiled tubing. In a cased hole, a barrier should be verified with a documented pressure or inflow test. During a pressure test, at least 500 psi above the injected pressure below the barrier but not exceed the casing strength minus the wear allowance in order to avoid damaging the primary cement. These practices and guidelines were adopted to qualify and demonstrate the use of a well barrier failure approach to assess the abandonment integrity of Karoo deep legacy abandoned wells. These industry practices and regulatory guidelines

were established to demonstrate well barrier elements (WBEs) of abandoned wells through segments that were improperly constructed and abandoned as per the [39,40,64] guidelines as demonstrated in Section 4.1 and Figure 6.

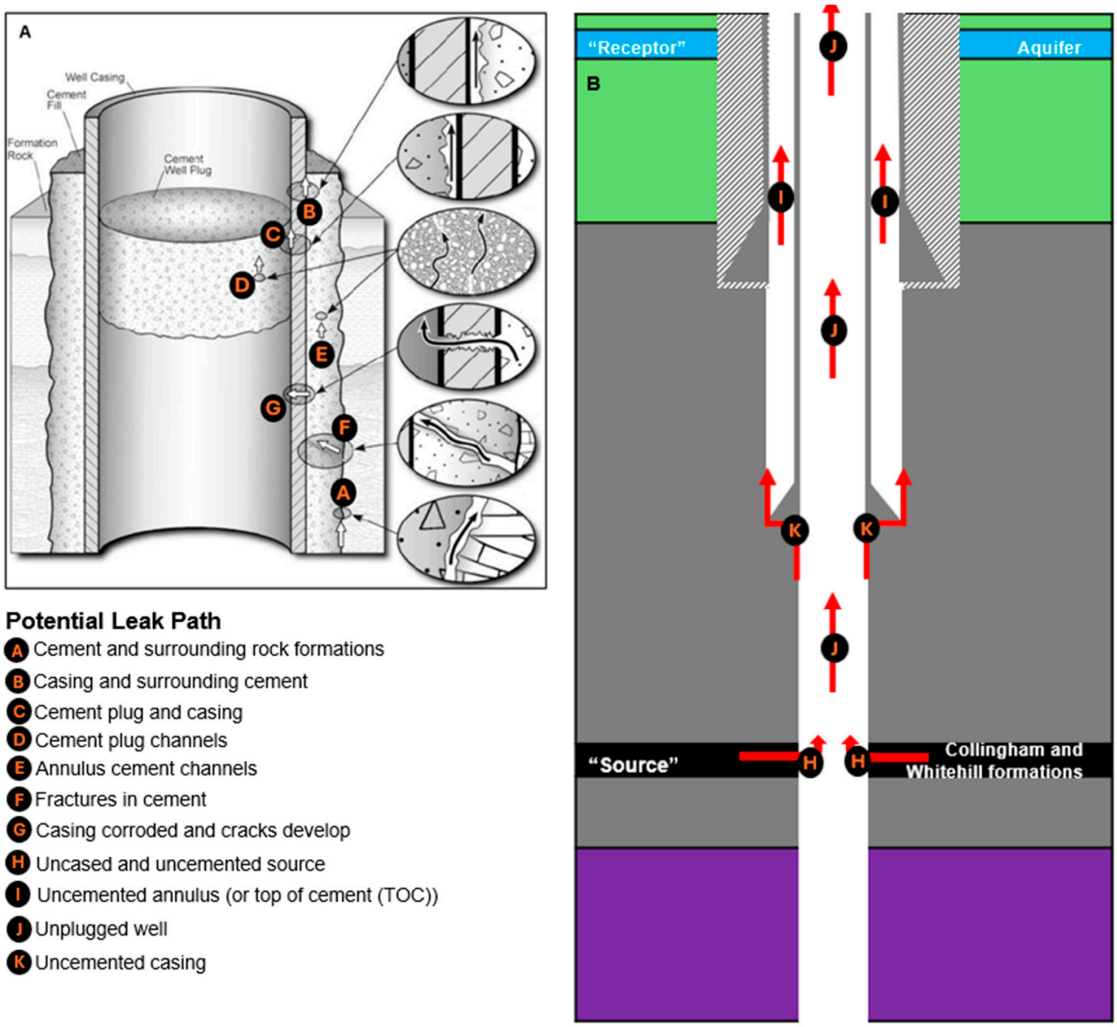


Figure 6. Schematic illustrations of the routes of a possible fluid leak in (**A**) a cemented wellbore barrier failure and (**B**) an uncemented wellbore barrier failure that provide pathways for fluid movement [65,66].

4. Data Collection and Analytical Procedures

4.1. Well Schematic Reconstruction

Data Collection

Well engineering data from completion reports were obtained from Petroleum Agency SA (PASA) and the Council for Geoscience (CGS). Of the 15 legacy wells in the study area, there are only 4 with drilling engineering data that demonstrate how the wells were constructed and abandoned. These wells are CR 1/68, KW 1/67, KA 1/65, and KDD, which were schematically reconstructed against the intersecting geological formations. Rock units known to host hydrocarbons ("sources") and portable groundwater ("receptors") were clearly marked in their associated groups in the Karoo supergroup, and potential leakage of fluids from the source to the receptor was denoted using arrows indicating migration pathways (Figure 6).

Figure 6 presents potential leak points on legacy abandoned wells identified based on completion reports assessed based on modern industry practices [64] and statutory

regulations [39,40] described in Section 3. Identified potential leak points are further described as follows:

(A) Cement and surrounding rock formations—poor cement and rock formation bonding due to loss of cement slurry in the surrounding rock fractures. According to [39,40] and [64] cement placement must be verified by leak of test (LOT) or cement bond log (CBL). These procedures were not performed on these wells which indicate non-compliance with [39,40] and [64] standard framework. Wells not verified according to these standards have high chances of leaking.

(B) Casing and surrounding cement—poor cement and casing bonding due to loss of cement slurry in the surrounding rock fractures. According to [39,40] and [64] cement placement must be verified by leak of test (LOT) or cement bond log (CBL). These procedures were not performed on these wells which indicate non-compliance with [39,40] and [64] standard framework. Wells not verified according to these standards have high chances of leaking.

(C) Cement plug and casing—poor bonding between the cement plug and the casing. According to [39,40] and [64], the placement of cement plug must be verified either by tagging or by conducting a weight test on a drill pipe or by using a wireline with coiled tubing. These procedures were not performed on these wells which indicate non-compliance with [39,40] and [64] standard framework. Wells not verified according to these standards have high chances of leaking.

(D) Cement plug channels—cement channels on cement plug. According to [39,40] and [64], the placement of cement plug must be verified either by tagging or by conducting a weight test on a drill pipe or by using a wireline with coiled tubing. These procedures were not performed on these wells which indicate non-compliance with [39,40] and [64] standard framework. Wells not verified according to these standards have high chances of leaking.

(E) Annulus cement channels—channel on annulus cement due to loss of cement slurry in the surrounding rock fractures. According to [39,40] and [64] cement placement must be verified by leak of test (LOT) or cement bond log (CBL). These procedures were not performed on these wells which indicate non-compliance with [39,40] and [64] standard framework. Wells not verified according to these standards have high chances of leaking.

(F) Fractures in cement between casing and rock formations—fractures that develop overtime between formation–cement–casing. According to [39,40] and [64] cement placement must be verified by leak of test (LOT) or cement bond log (CBL). These procedures were not performed on these wells which indicate non-compliance with [39,40] and [64] standard framework. Wells not verified according to these standards have high chances of leaking.

(G) Casing corrosion—corrosion that occurs on casing overtime. according to [39,40] and [64], free pipe has high chances to corrode and crack, which allows seepage into the wellbore and successive layers. Casing pipes must be cemented in place to prevent potential corrosion and leakage. Some casings were not cemented whereas others were not fully cemented on risky zones such as hydrocarbon bearing layers. According to these standard frameworks, such zones have high chances of leaking H_2S and CO_2 which have potential to corrode the pipe.

(H) Un-cased and uncemented sources—hydrocarbon source rock not cased and open to the wellbore. According to [39,40] and [64], zones with potential to leak hydrocarbons must be cased and cemented to prevent leakage. These procedures were not performed on these wells which indicate non-compliance with [39,40] and [64]

standard framework. Hydrocarbons sources not cased and cement have high chances of leaking into successive layers or wellbore.

(I) Uncemented section above the top of the cement—annulus sections not fully cement for shallow pressurized zones. According to [39,40] and [64] cement placement must be verified by leak of test (LOT) or cement bond log (CBL). These procedures were not performed on these wells which indicate non-compliance with [39,40] and [64] standard framework. Wells not verified according to these standards have high chances of leaking.

(J) Unplugged well—well abandoned without plugs. According to [39,40] and [64], when wells reach end of life, they must be abandoned with cement plugs to prevent well leakage into the successive layers. The cement plugs placed must be verified either by tagging or by conducting a weight test on a drill pipe or by using a wireline with coiled tubing. These procedures were not performed on these wells which indicate non-compliance with [39,40] and [64] standard framework. Wells not verified according to these standards have high chances of leaking.

(K) Uncemented casing—annulus sections not cemented at all. According to [39,40] and [64], after casing installation, the casings must be cemented in place to achieve zonal isolation and ensure integrity. Good isolation requires complete annular filling and tight cement interfaces with respect to the formations and casing. After cementing phase, the hole must be pressure-tested using a LOT and CBL to ensure there is no potential leakage. These procedures were not performed on these wells which indicate non-compliance with [39,40] and [64] standard frameworks. Wells not cemented and verified according to these standards have high chances of leaking.

Based on this dataset, schematic well structures and geological cross-sections were rendered using Surfer software and edited using Excel and Microsoft PowerPoint. Well completion reports were evaluated to accurately mark the depths of geological formation groups and indicate the source and receptor layers. In addition, the literature was reviewed further to ascertain the maturity of the Ecca group layers that have generated hydrocarbons. To verify host aquifer formations, reconnaissance was conducted to consult with farmers about the depths of their groundwater boreholes. Well completion reports were used to reconstruct the well layout with well barrier elements represented. Each drilled segment was reconstructed telescoping down, with hole depth, hole size, casing set, and cemented and plugged zones represented (Table 2). Locations of leaks/well failures as per [39,40] and [64] guidelines were documented as demonstrated in Figure 6.

Table 2. Well completion data for the construction and plugging statuses of abandoned wells.

Well	TD, Driller	Well Phase	Hole Sizes	Drilled Depth	Casing Size	Cased Depth	Grouting Depth	Plugs
KA 1/65	2600.6 m	Conductor	26″	9.7 m	Open hole	-	-	No plug
		Surface	17½″	187.4 m	13³/₈ ″	186.8 m	To surface	No plug
		Intermediate	12¼″	2327.7 m	9⁵/₈″	2302.4 m	To 2071.1 m	792.4 m 1865.3 m
		Production	8½″	2600.5 m	Open hole	-	-	No plug
CR 1/68	4657.9 m	Conductor	26″	19.8 m	20″	19.5 m	To surface	No plug
		Surface	17½″	158.4 m	13³/₈″	157.2 m	To surface	No plug
		1st Intermediate	12¼	2531.6 m	9⁵/₈″	2489.2 m	To 447.1 m	Surface 243.8
		2nd Intermediate	8½	4388.8 m	Open hole	-	-	2488.9 2743.2 m
		Production	6¾	4657.9 m	Open hole	-	-	4593.9 m

Table 2. *Cont.*

Well	TD, Driller	Well Phase	Hole Sizes	Drilled Depth	Casing Size	Cased Depth	Grouting Depth	Plugs
KW 1/67	5554.6 m	Conductor	26″	19.8 m	20″	19.5 m	To surface	No plug
		Surface	17½″	305.7 m	13 3/8″	304.7 m	To surface	No plug
		1st Intermediate	12¼″	3049.5 m	9 5/8″	3048.6 m	Not mentioned	No plug
		2nd Intermediate	8½″	5216 m	Open hole	-	-	No plug
		Production	6¾″	5554 m	Open hole	-	-	No plug
KDD	2978.82 m	Conductor	Not mentioned	Not mentioned	Not mentioned	Not mentioned	Not mentioned	Not mentioned
		Surface	PQ	950 m	Unidentified	950 m	To surface	No plug
		Intermediate	HQ	1750 m	Unidentified	1750 m	-	No plug
		Production	NQ	2978.82 m	Open hole	-	-	No plug

4.2. Geochemical Sampling and Analyses

4.2.1. Field Sampling

To help ensure representative groundwater samples were collected, we employed a temperature, level, and conductivity (TLC) meter and a multiparameter probe at each site to determine when the water being sampled was representative of the targeted aquifer. For unequipped boreholes, bailers were used to extract the groundwater and water levels were measured with the TLC meter. For fully equipped boreholes, samples were collected directly from the pipes linked to the borehole heads, and depth information was obtained from farmer records. IsoFlasks® were used to collect groundwater for dissolved molecular gas and isotope analyses.

To help determine whether gas from deep wells had leaked into shallow aquifers, 14 abandoned deep well sites were investigated. Four of these wells were sampled, while 10 could not be accessed. Additionally, 46 groundwater boreholes were sampled proximally to the 14 abandoned deep wells. This led to a total of 50 groundwater samples collected across the study area. All the groundwater boreholes sampled are currently in use for household and agricultural activities.

4.2.2. Laboratory Analyses

Dissolved gas samples were analyzed at the Stratum Reservoir (Isotech) laboratory in Champaign, Illinois, USA. The samples were analyzed for gas component concentrations using a gas chromatograph (GC) (manufactured in 2010, Shimadzu, Kyoto, Japan). Gas was exsolved by injecting helium into the IsoFlasks to form a headspace and then placing the IsoFlasks on a shaker for a minimum of 2 h to allow equilibration of the dissolved gas between the water and the headspace. Afterwards, a syringe was used to extract the exsolved gas from the headspace in the IsoFlask and inject it into the GC. Fixed gases (hydrogen, argon, oxygen, and nitrogen) were quantified via a thermal conductivity detector, and carbon dioxide and hydrocarbon gases (methane, ethane, ethene, propane, propene, isobutane, n-butane, isopentane, n-pentane, and hexanes+) were quantified via a flame ionization detector.

Isotopic analysis was completed for samples with a dissolved hydrocarbon gas concentration of $\geq$ 0.05% methane for $\delta^{13}C_1$ and 0.24% methane for δDC_1. Ethane concentrations of > 0.02% are required to complete $\delta^{13}C_2$ analyses. Isotope data reported in black font were generated using the off-line method and have precisions of ±0.1‰ for $\delta^{13}C_1$ and ±3.5‰ for δDC_1 (Table 3). Isotope data reported in red font were generated using the online method and have precisions of ±0.3‰ for $\delta^{13}C_1$ and $\delta^{13}C_2$ and ±5‰ for δDC_1 (Table 3).

Table 3. Dissolved gas concentrations and isotopic compositions and concentrations of dissolved methane, ethane, and propane.

Isotech	Sample	Field	Location	Sampling	$\delta^{13}C_1$	δDC_1	$\delta^{13}C_2$	Dissolved CH_4		Dissolved C_2H_6		Dissolved C_3H_8	
Lab No.	Name	Name		Point	‰	‰	‰	cc/L	mg/L	cc/L	mg/L	cc/L	mg/L
872238	BH01 B390	B390/1	Ceres	Blaawbosch Kalk	−60.05	−210.9		8.8	5.9	0.0002	0.0003	<0.0002	<0.0004
872239	BH02 B390	B390/1	Ceres	Blaawbosch Kalk	−51.6	−164		0.89	0.60	<0.0003	<0.0003	<0.0003	<0.0005
872240	BH03 B390	B390/1	Ceres	Blaawbosch Kalk				0.0098	0.0065	<0.0003	<0.0004	<0.0003	<0.0006
872241	BH 01 SA	SA 1/66	Merweville	Sambokraal				0.0052	0.0035	<0.0003	<0.0004	<0.0003	<0.0005
872242	BH 02 SA	SA 1/66	Merweville	Sambokraal				<0.0006	<0.0004	<0.0003	<0.0004	<0.0003	<0.0005
872243	BH 03 SA	SA 1/66	Merweville	Sambokraal	−40.6	−113		0.61	0.41	0.0013	0.0016	<0.0002	<0.0004
872244	KDD	KDD	Beaufort West	Beaufort West	−30.39	−245.7	−36.7	16	11	0.32	0.40	0.010	0.019
872245	BO4H-BW	KDD	Beaufort West	Beaufort West				0.067	0.045	<0.0003	<0.0004	<0.0003	<0.0005
872246	BO2H-BW	KDD	Beaufort West	Beaufort West				0.0015	0.00098	<0.0002	<0.0003	<0.0002	<0.0004
872247	SPF-BW	KDD	Beaufort West	Beaufort West				0.0056	0.0037	<0.0003	<0.0003	<0.0003	<0.0005
872248	BH01KW	KW 1/67	Prince Albert	Klein Waterval				0.0052	0.0034	<0.0002	<0.0002	<0.0002	<0.0003
872249	BH02KW	KW 1/67	Prince Albert	Klein Waterval				0.0093	0.0062	<0.0003	<0.0003	<0.0003	<0.0005
872250	BH01VR	VR 1/66	Graaff Reinet	Vrede				0.0004	0.0003	<0.0002	<0.0003	<0.0002	<0.0004
872251	BH02VR	VR 1/66	Graaff Reinet	Vrede				0.050	0.034	<0.0003	<0.0003	<0.0002	<0.0004
872252	BH03VR	VR 1/66	Graaff Reinet	Vrede				<0.0005	<0.0003	<0.0003	<0.0003	<0.0003	<0.0005
872253	BH04VR	VR 1/66	Graaff Reinet	Vrede	−45.02	−183.0		19	13	0.00075	0.00094	<0.0004	<0.0007
872254	BH01SC	SC 3/67	Aberdeen	Skietfontein				0.041	0.027	0.00042	0.00052	<0.0002	<0.0004
872255	BH02SC	SC 3/67	Aberdeen	Skietfontein				0.097	0.065	0.00100	0.0012	<0.0003	<0.0006
872256	BH03SC	SC 3/67	Aberdeen	Skietfontein				0.0080	0.0053	<0.0003	<0.0004	<0.0003	<0.0005
872257	BH04SC	SC 3/67	Aberdeen	Skietfontein				0.0034	0.0023	<0.0003	<0.0003	<0.0003	<0.0005
872258	BH05SC	SC 3/67	Aberdeen	Skietfontein				0.0016	0.0011	<0.0002	<0.0003	<0.0002	<0.0004
872259	BH01KA	KA 1/65	Murraysburg	Karee Bosch	−29.96	−203.3	−25.3	24	16	0.16	0.20	0.00085	0.0016
872260	BH02KA	KA 1/65	Murraysburg	Karee Bosch				0.068	0.046	<0.0005	<0.0006	<0.0005	<0.0008
872261	BH03KA	KA 1/65	Murraysburg	Karee Bosch				0.037	0.025	<0.0004	<0.0005	<0.0004	<0.0007
872262	KA 1/65	KA 1/65	Murraysburg	Karee Bosch	−27.85	−220.3	−35.1	17	11	0.46	0.58	0.020	0.037
872263	BH01AB	AB 1/65	Victoria West	Abrahamskraal				0.091	0.061	0.0012	0.0015	<0.0003	<0.0005
872264	BH02AB	AB 1/65	Victoria West	Abrahamskraal				0.0039	0.0026	<0.0003	<0.0003	<0.0003	<0.0005

Table 3. *Cont.*

Isotech	Sample	Field	Location	Sampling	$\delta^{13}C_1$	δDC_1	$\delta^{13}C_2$	Dissolved CH_4		Dissolved C_2H_6		Dissolved C_3H_8	
Lab No.	Name	Name		Point	‰	‰	‰	cc/L	mg/L	cc/L	mg/L	cc/L	mg/L
872265	BH 01 KD	KD 1/71	Carnarvon	Heuwels				0.0048	0.0032	<0.0003	<0.0004	<0.0003	<0.0005
872266	BH 02 KD	KD 1/71	Carnarvon	Heuwels				<0.0006	<0.0004	<0.0003	<0.0004	<0.0003	<0.0005
872267	BH 03 KD	KD 1/71	Carnarvon	Heuwels				0.0091	0.0061	<0.0002	<0.0003	<0.0002	<0.0004
872268	BH 04 KD	KD 1/71	Carnarvon	Heuwels				<0.0004	<0.0003	<0.0002	<0.0003	<0.0002	<0.0004
872269	BH01AM	AM1/70	Williston	Amersfontein				0.013	0.0085	<0.0003	<0.0003	<0.0003	<0.0005
872270	BH02AM	AM1/70	Williston	Amersfontein				0.0031	0.0021	<0.0005	<0.0006	<0.0004	<0.0008
872271	BH03AM	AM1/70	Williston	Amersfontein				0.0013	0.00088	<0.0003	<0.0003	<0.0003	<0.0005
872272	BH04AM	AM1/70	Williston	Amersfontein				0.00093	0.00062	<0.0002	<0.0003	<0.0002	<0.0004
872273	BH01KC	KC 1/71	Calvinia	Kwaggasfontein	−63.4			0.19	0.13	<0.0002	<0.0003	<0.0002	<0.0004
872274	BH02KC	KC 1/71	Calvinia	Kwaggasfontein				0.0033	0.0022	<0.0003	<0.0004	<0.0003	<0.0006
872275	BH03KC	KC 1/71	Calvinia	Kwaggasfontein				0.0007	0.0004	<0.0002	<0.0003	<0.0002	<0.0004
872276	BH04KC	KC 1/71	Calvinia	Kwaggasfontein				<0.0006	<0.0004	<0.0003	<0.0004	<0.0003	<0.0006
872277	Qu 1/65	Qu 1/65	Frasersburg	Quaggasfontein	−18.27	−227.9	−22.3	13	8.5	0.13	0.17	0.018	0.032
872278	BH01Qu1	Qu 1/65	Frasersburg	Quaggasfontein				0.0029	0.0019	<0.0003	<0.0004	<0.0003	<0.0005
872279	BH02Qu1	Qu 1/65	Frasersburg	Quaggasfontein				0.0052	0.0035	<0.0002	<0.0003	<0.0002	<0.0004
872280	BH03Qu1	Qu 1/65	Frasersburg	Quaggasfontein				0.0005	0.0003	<0.0003	<0.0003	<0.0003	<0.0005
872281	BH04Qu1	Qu 1/65	Frasersburg	Quaggasfontein				0.030	0.020	<0.0003	<0.0003	<0.0002	<0.0004
872282	BH 01 Qu2	Qu 2/65	Frasersburg	Beeswater				0.024	0.016	0.0003	0.0003	0.00052	0.00096
872283	BH 02 Qu2	Qu 2/65	Frasersburg	Beeswater				0.026	0.018	0.0005	0.0006	<0.0005	<0.0009
872284	BH 03 Qu2	Qu 2/65	Frasersburg	Beeswater	−50.14	−334		2.9	2.0	0.0004	0.0005	<0.0004	<0.0008
872285	BH 04 Qu2	Qu 2/65	Frasersburg	Beeswater				0.0032	0.0022	<0.0003	<0.0004	<0.0003	<0.0006
872286	BH 05 Qu2	Qu 2/65	Frasersburg	Beeswater				0.0004	0.0003	<0.0002	<0.0003	<0.0002	<0.0004
872287	KL 1/65	KL 1/65	Sutherland	Klip Drift	−29.60	−240.0	−31.3	13	8.8	0.22	0.28	0.0094	0.017

All gas component carbon isotope values are reported on a scale defined by a two-point calibration of LSVEC and NBS 19. No isotope analyses means insufficient analyte for isotope analysis. In red = isotopes obtained online via GC-C-IRMS or GC-P-IRMS.

Most of the isotopic analyses were performed by using traditional offline sample preparation techniques and subsequently taking dual-inlet mass spectrometric $^{13}C/^{12}C$ measurements using a Finnigan MAT Delta S Isotope Ratio mass spectrometer. $^{2}H/^{1}H$ measurements were performed using a Finnigan Delta Plus XL isotope ratio mass spectrometer. Sample results were compared with accepted reference standards (NGS #1, #2, or #3); isotope-ratio determinations involved multiple direct comparisons of the sample to the reference standard (generally at least six comparisons). Stable carbon and hydrogen isotope compositions are reported in delta (δ) notation, which is the difference between the ratios of the two isotopes of interest in the sample and the ratio in an international reference standard. That is,

$$\delta X\text{sample} = [(R\text{sample} - R\text{standard})/R\text{standard}] \times 1000 \quad (1)$$

where X represents the isotope of interest, in this case ^{13}C and ^{2}H or deuterium (D), and R represents the ratio of $^{13}C/^{12}C$ or $^{2}H/^{1}H$. The value is expressed per mil (‰), equivalent to parts per thousand.

4.3. Data Limitations

Of the fifteen deep wells investigated, only four have well completion reports (KA 1/65, CR 1/68, KW 1/67, and KDD). Due to the majority of wells not having completion reports it was challenging to assess abandonment integrity and evaluate the cost for re-plugging the remedial measure. Innovative research is required to improve this work and to encourage research. This study also acknowledges that of fifteen deep wells investigated, only four have been sampled (KDD, KA 1/65, Qu 1/65, and KL 1/65), and the results were inferred to other eleven deep wells not sampled. This hypothetical assumption may be improved by future research with potential new innovative ideas. Such ideas may suggest different observations compared to this study.

5. Results and Interpretation

5.1. Assessing Well Schematic Diagrams and Integrity

5.1.1. Well Construction, Plugging, and Abandonment

Well KA 1/65 was drilled as presented in Table 2 and demonstrated in Figure 7. The conductor phase was not cased, thus increasing near-surface leakage. The surface and intermediate phases were cased with $13^{3}/_{8}''$ and $9^{5}/_{8}''$ casings and grouted in place. The grout in the surfa^{3}/$_{8}$e casing ($13^{3}/_{8}''$) was circulated to the surface, filling the entire annulus space between the conductor-drilled phase and the surface casing. During the intermediate phase, grout was circulated to 2071.1 m, leaving the annulus above uncemented and creating a potential migration pathway. The production phase was completed barefoot. The well was completed with two open spaces: an uncemented annulus portion in the intermediate phase and an open-hole completion in the production phase. Though this well had two open spaces, three (3) cement plugs (Plugs A, B, and C) were set in $9^{5}/_{8}''$ intermediate casing when the well was abandoned. No verification work indicating whether the plugs met barrier length/verification standards (NORSOK D-010/ISO 16530-2) could be found. During drilling, well KA 1/65 intersected rocks of the Karoo supergroup (the Beaufort, Ecca, and Dwyka groups) and the pre-cape formation of Nama-Natal province. After drilling, the well was tested for hydrocarbons but proved non-commercial; however, traces of methane, ethane, and propane were recorded. These hydrocarbon components were entirely related to shales intersected at 749.8 m, 1219.2 m, and 2154.9 m depths and are denoted as sources C, B, and A, respectively, in Figure 7. Due to improper well construction and abandonment of this well, these hydrocarbons and other associated fluids are expected to leak into the shallow groundwater aquifer.

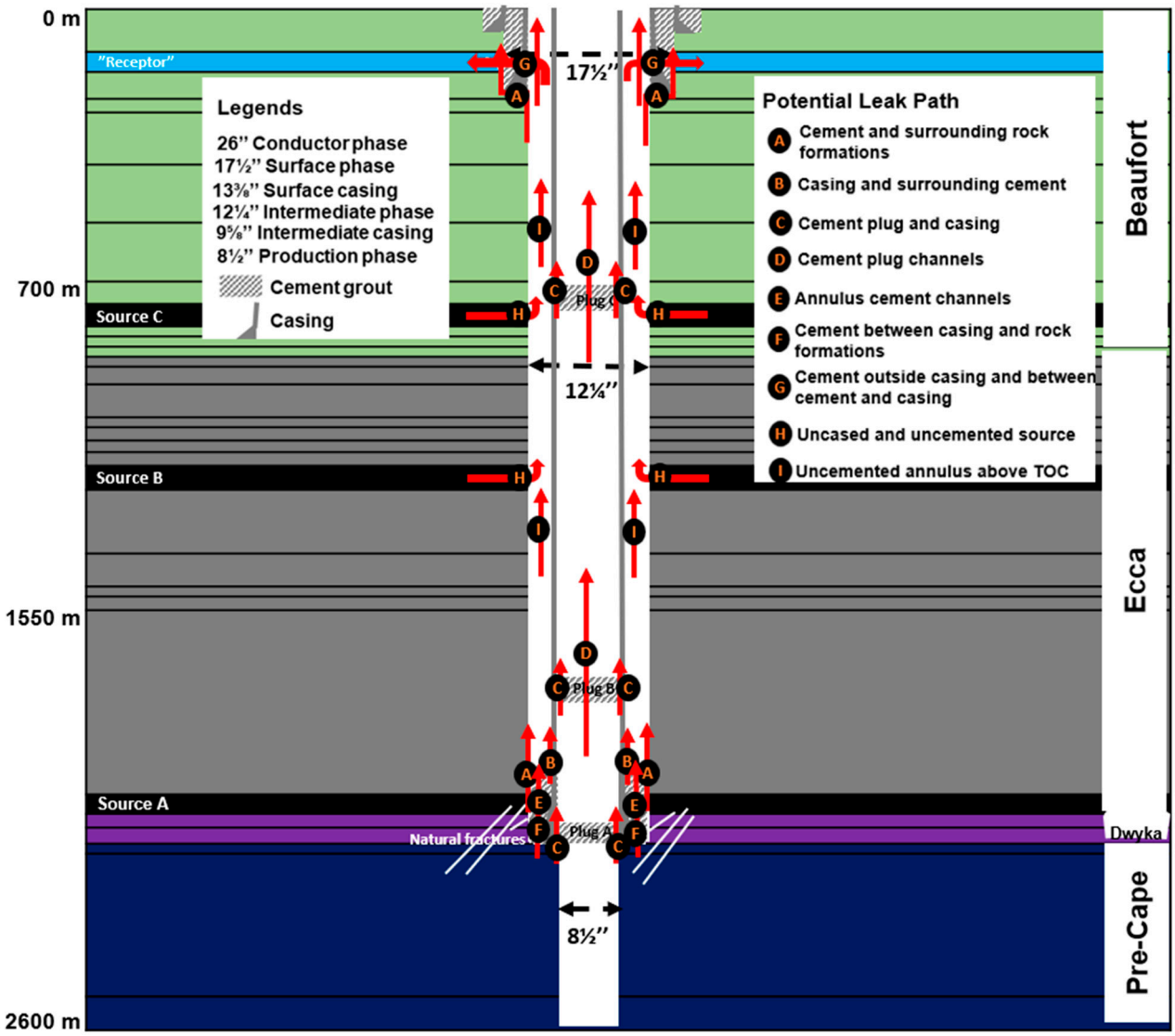


Figure 7. Schematic representation of Well KA 1/65 drilled through the Beaufort, Ecca, Dwyka, and pre-Cape formations, indicating well construction and abandonment status, identifying the potential leak paths, and how hydrocarbon gas could flow to shallower units (red arrows).

Well CR 1/68 was drilled as presented in Table 2 and demonstrated in Figure 8. The conductor, surface, and intermediate phases were cased with 20″, 13$^{3}/_{8}$″, and 9$^{5}/_{8}$″ casings, respectively. The conductor and surface phases were grouted to the surface. In contrast, during the intermediate phase, the grout was circulated to 447.1 m, leaving the annulus above uncemented and creating a potential migration pathway. The second intermediate and production phases were completed in an open-hole fashion. Overall, the well was completed with three open spaces: the two open-hole completions of the second intermediate and production phases and the uncemented top section of the first intermediate phase. Though this well was completed with three open spaces, five cement plugs (Plugs A, B, C, D, and E) were set on a 6¾ production phase, an 8½ second intermediate phase, a 9$^{5}/_{8}$″ first intermediate casing, a 13$^{3}/_{8}$″ surface casing, and a 20″ conductor casing to abandon the well. There were no verification tests indicating whether the plugs met barrier length/verification standards (NORSOK D-010/ISO 16530-2). Well CR 1/68 intersected rocks of the Karoo supergroup (the Beaufort, Ecca, and Dwyka groups) and the Cape supergroup. After drilling, this well was tested for the presence of oil and potential economic flow rate, and it was determined to be uneconomical; however, hydrocarbon indications

were confirmed, consisting of minor occurrences of methane, ethane, and propane at various levels of the well. These hydrocarbon compounds were detected between 2322.2 and 2369.8 m, 2485.3 and 2533.4 m, 2900 and 3548.4 m, 4492.7 and 4593.9 m, and 4593.9 and 4657.9 m intervals and are marked as sources E, D, C, B, and A, respectively, in Figure 8.

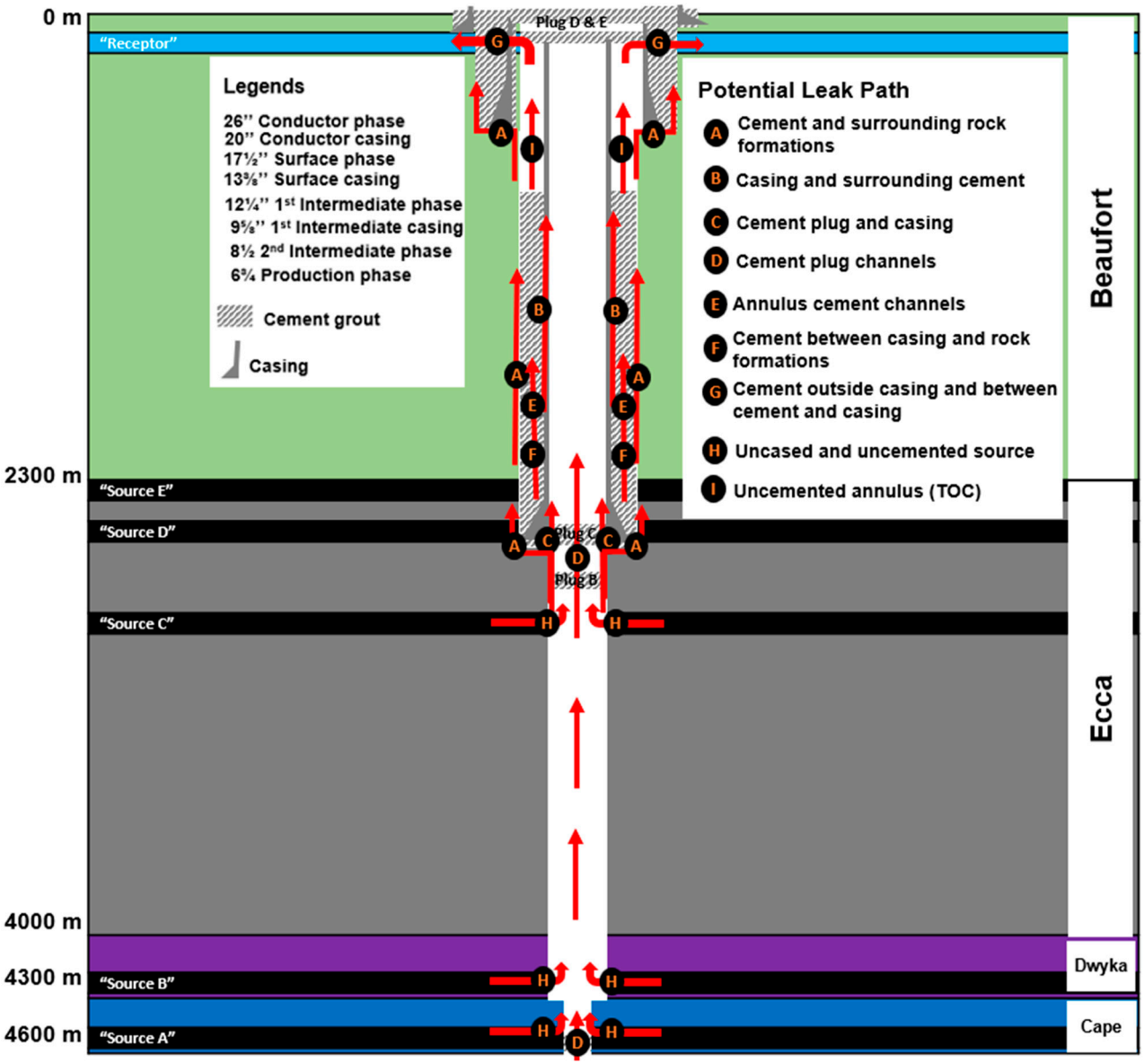


Figure 8. Schematic representation of Well CR 1/68 drilled through the Beaufort, Ecca, Dwyka, and Cape formations, indicating well construction and abandonment status and identifying the potential leak paths.

Well KW 1/67 was drilled as presented in Table 2 and demonstrated in Figure 9. The conductor and surface phases were cased and grouted in place. The grout in the conductor and surface casings was circulated to the surface, whereas grouting in the intermediate casings was incomplete, leaving the annulus above uncemented and creating a potential migration pathway. Both the second intermediate and production phases were completed in an open-hole manner. The well was completed with two known open spaces in the second intermediate and production phases. Upon well completion, two cement plugs were attempted at 5242.5 m and 5303.5 m, but they failed to set due to the loss of cement that leaked through faults and fractures. The well was abandoned without plugs (Figure 9).

This project proved to be a well barrier failure for plugging as per the NORSOK D-010/ISO 16530-2 standards. Well KW 1/67 intersected rocks of the Karoo supergroup (the Beaufort, Ecca, and Dwyka groups) and the Cape supergroup (Figure 9). After drilling, this well was tested for oil, but no economic flow rate was observed. The test results showed there was about 1455 ppm of fluorescent hydrocarbon liquid. These liquid hydrocarbons were held in impermeable shale rock, as no recovery could be achieved. In the end, the well was considered uneconomic, but it was assumed that if the shales were fractured, they would be regarded as both source rock and reservoir rock. Despite the oil results, the well tested positive for gas, with the best recovery occurring over the fault zone and other minor occurrences in the carbonaceous rock that do not represent an economic flow of methane. It was concluded that the well was dry due to a lack of commercial flow, with only minor gas shows. This well was abandoned with no plugs and has a high potential for leaking hydrocarbons into the atmosphere.

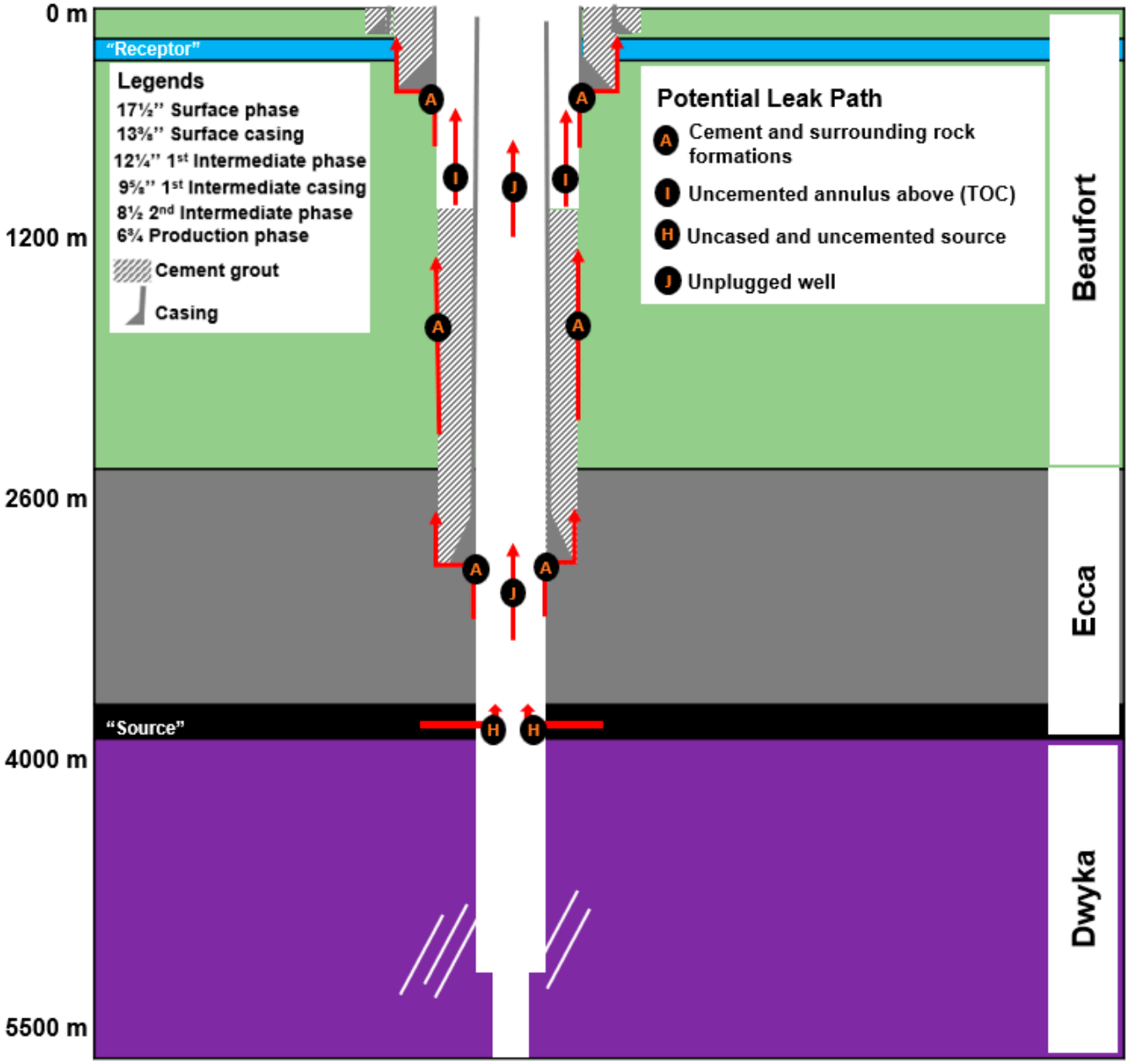


Figure 9. Schematic representation of KW 1/67 drilled through the Beaufort, Ecca, and Dwyka formations, indicating well construction and abandonment status and the potential leak paths identified.

Well KDD was drilled as presented in Table 2 and demonstrated in Figure 10. The conductor and surface phases were cased and grouted in place. The intermediate phase was cased and not cemented, creating a potential migration pathway. The production phase was completed in an open-hole manner. In conclusion, this well was abandoned without plugs (Figure 9). This attempt proved to be a well barrier failure regarding plugging as per the NORSOK D-010/ISO 16530-2 standards. Well KDD intersected rocks of the Karoo supergroup (the Beaufort, Ecca, and Dwyka groups). After drilling, core samples were collected from the Whitehill and Collingham formations for desorption analysis, and the results showed the presence of methane, ethane, and propane. The desorption analysis zone was identified as the source, as shown in Figure 10. Due to improper well construction and abandonment, the tested hydrocarbons may be released from the source, leaking into shallow groundwater and the atmosphere.

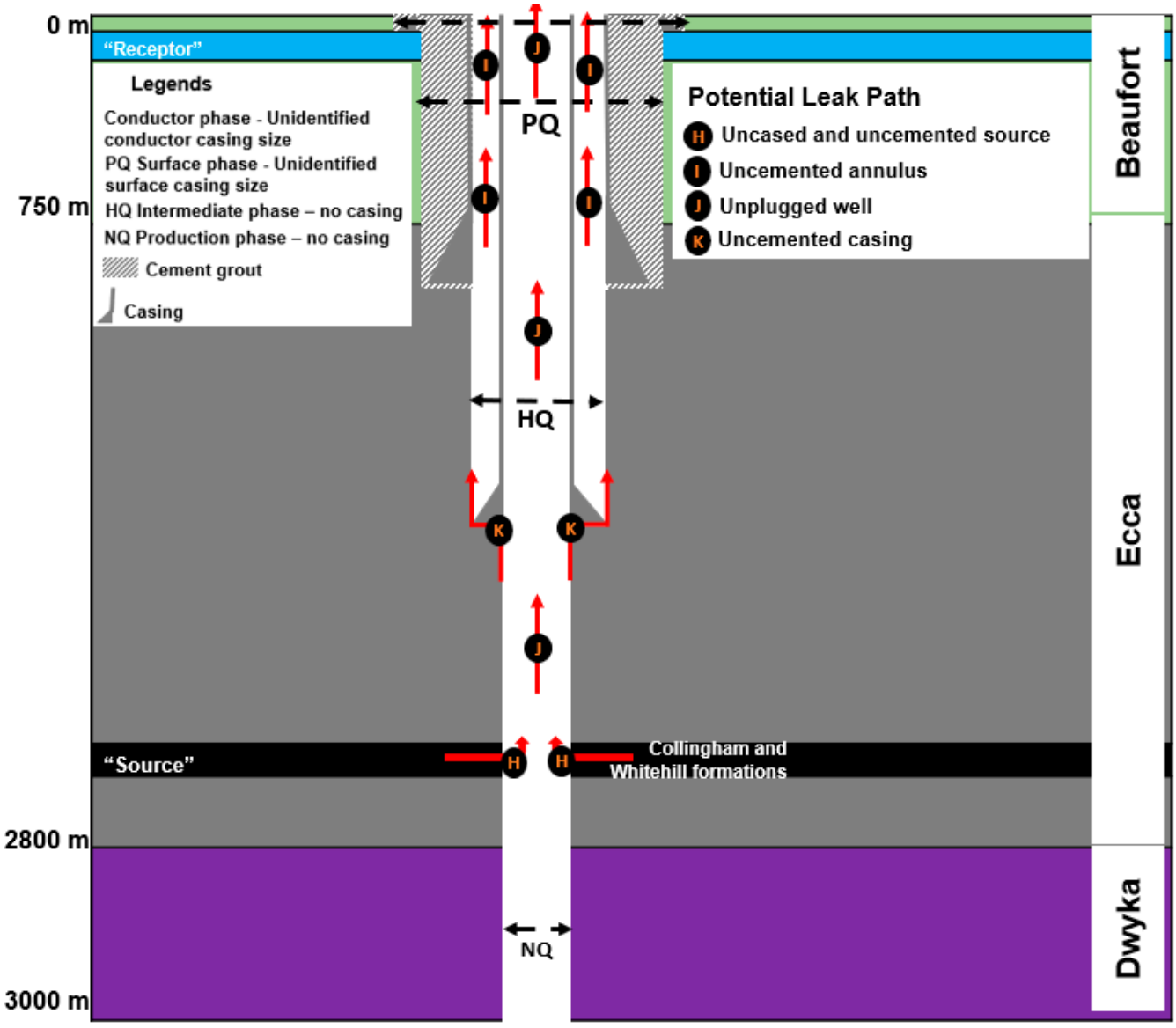


Figure 10. Schematic representation of Well KDD drilled through the Beaufort, Ecca, and Dwyka formations, indicating well construction and abandonment status and identifying the potential leak paths.

5.1.2. Assessment of Potential Leakage and Migration

All the sketches demonstrated well barrier failures, indicating improper construction and abandonment that failed to adhere to oil-and-gas industry practices [64] and statutory regulations [39,40]. Figures 7–10 demonstrate potential well barrier failures with up to eleven possible leak paths linked to improper construction and abandonment. These wells have intersected zones of hydrocarbon gas bearing rock units with the potential to leak. For wells KA 1/65 and CR 1/68, records from completion reports indicate that cement circulation was insufficient for plugging the wells due to loss of cement slurry to natural fractures. Insufficient circulation of cement for plugging these wells increases the risk of well leakage, and such failure could be associated with leak paths C and D (Figures 7 and 8). In well KW 1/67, no plug had been set, and it was abandoned without a plug. Similarly, the KDD well was abandoned without cement plugging. The failure of the cement to set in KW 1/67 and the failure of cement plugging in KDD increase the risk of leakage into the atmosphere (Leak path J). Poor cement circulation was also encountered during casing grouting, leading to poor bonding between the cement and rock formations (Leak Path A), cement channels (Leak Path E), and cement and casing (Leak Path B). These leak paths are well demonstrated in Figures 7–9. Failure of the cement to set between the casing and rock formations creates cement channels, increasing the potential risk of well leakage. The annulus of the intermediate casing in wells KA 1/65, CR 1/68, and KW 1/67 was partially grouted, whereas the intermediate casing in the KDD well was not grouted, exposing the intermediate casings in these wells to corrosion. Over time, the casing corrodes and cracks develop, increasing the risk of potential well leakage (Leak Paths F and G in Figure 6). Intersected hydrocarbon sources in all wells were not cased and cemented (Leak Path H), allowing possible direct leakage into the wellbore in wells KW 1/67 and KDD and into the uncemented annulus of wells KA 1/65 and CR 1/68 (Leak Path I). The KDD intermediate casing was not cemented at all, and the failure to cement the well was identified as Leak Path K (Figure 10). Assessment of the completion reports indicated that no verification tests had been conducted to assess the integrity of the cement jobs. This means cement bond logs, mechanical or formation tests to verify the integrity of casing cement jobs, and tagging to verify the integrity of the cement plugs were not conducted. There was no indication that mud had been cleared in these wells before the cementation, and poor mud clearance also led to poor rock-to-cement bonding.

5.1.3. Extrapolation to Wells Without Completion Reports

Given the poor construction/abandonment practices observed in the documented wells, it is likely that the undocumented wells drilled by the same operator also exhibit deficiencies. This assumption was tested by sampling groundwater boreholes proximal to these wells for evidence of stray gas migration.

5.2. Geochemical Tracing of Stray Gas Leakage

5.2.1. Dissolved Concentrations of Methane, Ethane, and Propane

The results regarding dissolved stray gas concentrations across the study area are presented in Figure 11 and Table 3 below. Most samples (44 of 50) contained methane concentrations below the PA-DEP action level of 7 mg/L, while 6 exceeded this threshold, with values ranging from 8.5 mg/L in Fraserburg to 16 mg/L in Murraysburg. Although these levels are below the explosion risk threshold (~28 mg/L), they warrant monitoring and isotopic analysis to determine whether the gas is biogenic or thermogenic.

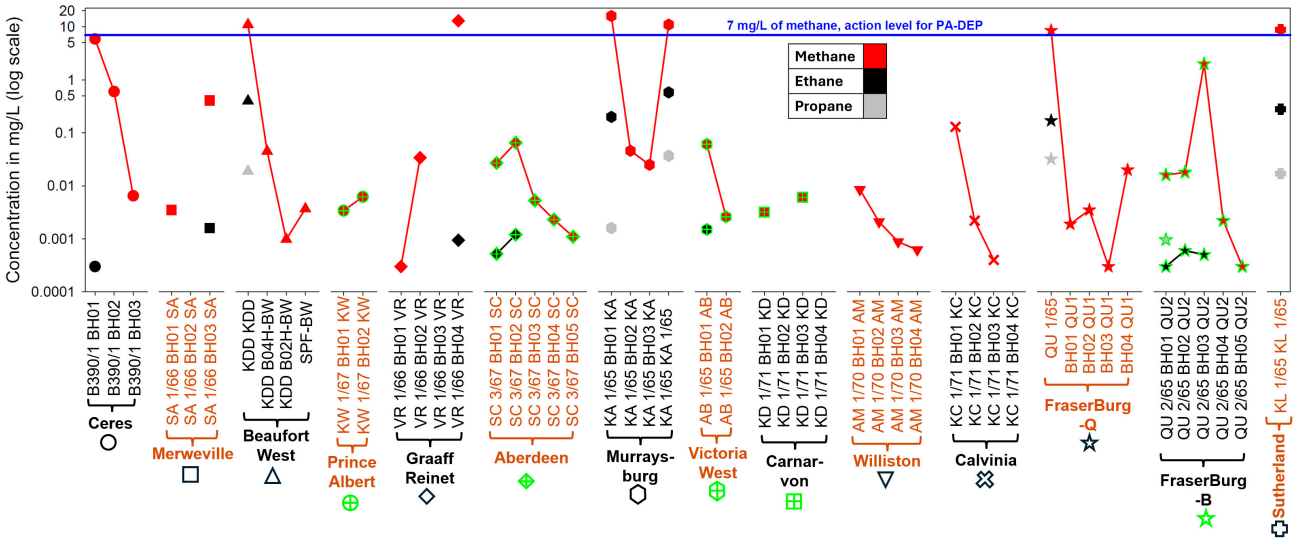


Figure 11. Methane (red symbols), ethane (black symbols), and propane (gray symbols) dissolved gas concentrations for each site. Data are grouped by location, and the symbol representing each location is shown at the bottom of the diagram. Data are displayed only for samples above the reporting limits, and the blue horizontal line represents the 7 mg/L methane action level set by the Pennsylvania Department of Environmental Protection (PA-DEP, Harrisburg, PA, USA).

5.2.2. Dissolved Gas $\delta^{13}C$ and δD Isotopic Analysis

Interpretation and Analysis

Of the 50 samples collected, only 11 contained sufficient hydrocarbon concentrations for isotopic analysis. At the Ceres location, only samples BH01B390 and BH02B390 had a sufficient dissolved gas concentration for isotopic analysis (Figure 11 and Table 3). The isotopic composition of BH01B390 suggests the hydrocarbon gas is primarily microbial, produced via the CO_2-reduction pathway, which is typically associated with subsurface groundwater environments (Figure 12).

These findings are consistent with very little ethane or heavier alkanes associated with BH01B390. The isotopic composition of BH02B390 is like that expected for thermogenic gas. However, the isotopic composition of the methane for BH02B390 could be the result of partial oxidation of gas that initially (prior to oxidation) had an isotopic composition like that of BH01B390. The effects of partial oxidation are shown by the bold, dashed arrow in the lower right of Figure 12. If one traces the dashed oxidation arrow back from the BH02B390 sample (envisioning what the isotopic composition of BH02B390 was prior to oxidation), it will fall relatively close to or on top of BH01B390, indicating that the gas in BH02B390 could be oxidized methane that originally formed via the same CO_2-reducing methanogenesis process that formed the gas in BH01B390.

A comparison of the methane/(ethane + propane) [$C_1/(C_2 + C_3)$] ratio versus the $\delta^{13}C$ of methane (referred to as a Bernard Plot) is often used to evaluate different gas sources. High ratios of $C_1/(C_2 + C_3)$ have characteristically been associated with microbial gas. For example, ratios of $C_1/(C_2 + C_3)$ above 1000 are considered primarily microbial gas; thermogenic gas typically has $C_1/(C_2 + C_3)$ ratios less than 50; and intermediate values (50–1000) may indicate mixed gas or altered migration [68–70]. The BH01B390 sample from Ceres had a $C_1/(C_2 + C_3)$ ratio of about 38600. Combining the $C_1/(C_2 + C_3)$ ratio with $\delta^{13}C$ for BH01B390 supports the conclusion that the gas in BH01B390 is primarily microbial (Figure 13).

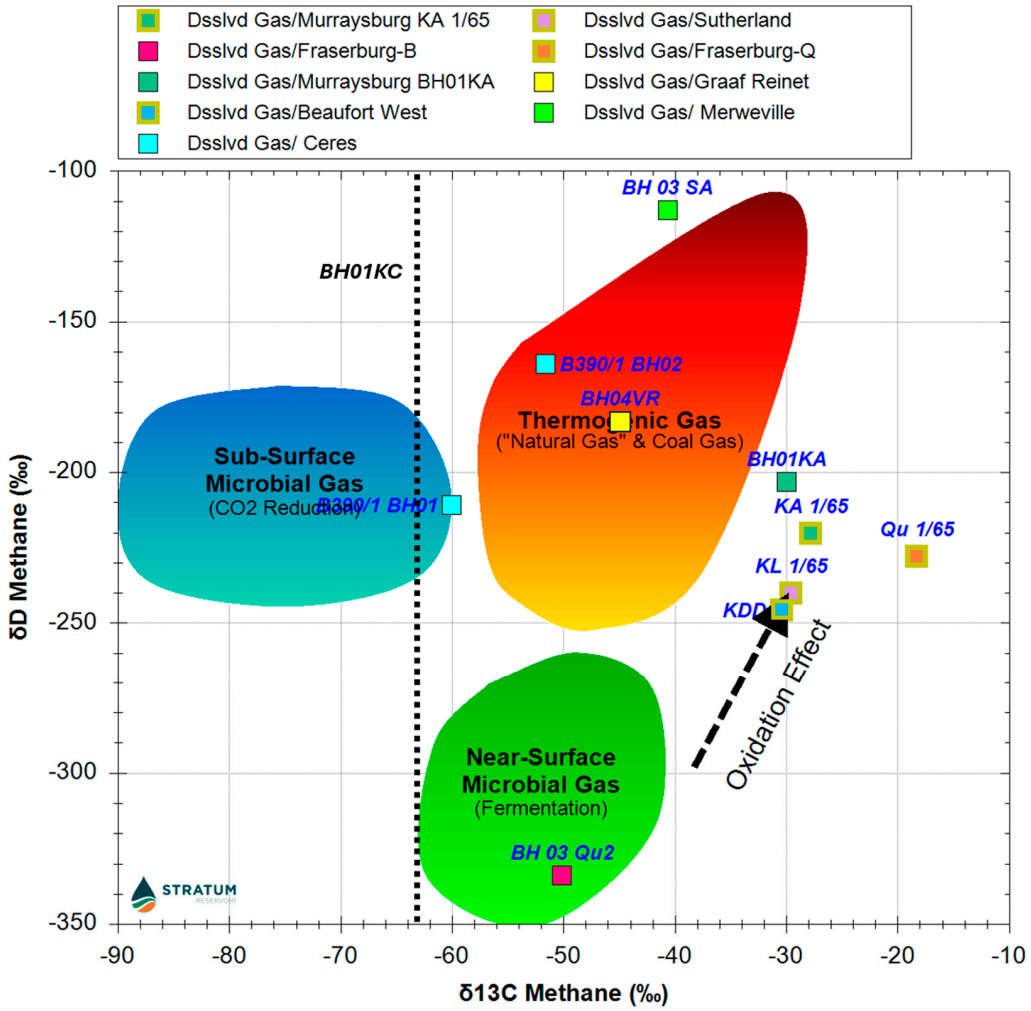


Figure 12. Graph of the $\delta^{13}C$ versus δD for the methane from the dissolved gas samples collected from the boreholes/deep wells across the study area. The bold, dashed arrow in the lower-right corner of the diagram shows the typical trend observed for the partial oxidation of methane (Diagram template based on [67]). The black dotted vertical line represents the $\delta^{13}C$ of methane for the BH01KC sample collected from Calvinia (insufficient methane concentrations for δD of methane analysis). The gold outline on datapoints represents samples with isotopic reversals ($\delta^{13}C$ of methane > $\delta^{13}C$ of ethane).

The dissolved gas sample BH02B390 contained 2.54% methane in the gas phase (Figure 11 and Table 3) but less than the reportable detection limit (1 ppm) for ethane and propane. Such low concentrations of ethane and propane are consistent with what would be expected for microbial gas. For example, if a range of values for the ethane and propane components is used (e.g., from the detection limit to half the detection limit) to calculate the $C_1/(C_2 + C_3)$ ratio for BH02B390, the obtained ratios would be approximately 12,700 to 25,400, respectively. These are high $C_1/(C_2 + C_3)$ ratios, making it likely that the methane in BH02B390 is also primarily microbial gas, which has probably undergone some partial oxidation, shifting the isotopic composition ($\delta^{13}C$) to more positive values compared to the value observed for BH01B390 (Figure 12).

In Merweville, only BH03SA had a dissolved gas concentration high enough for isotopic analysis (Figure 11 and Table 3). The $\delta^{13}C$ and δD compositions of methane for BH03SA fall within the range expected for thermogenic gas, depending on the template used for the $\delta^{13}C$-δD plot (Figure 12). It is not clear if the dissolved gas from BH03SA is of thermogenic or microbial origin or some combination of the two. The methane isotopic

composition for BH03SA may be related to partial oxidation effects in predominantly microbial gas. The impact of partial oxidation on the methane isotopic composition is indicated by the bold dashed arrow in Figure 12. The BH03SA sample from Merweville had a $C_1/(C_2 + C_3)$ ratio of about 509. This is greater than typically expected for thermogenic gas but less than expected for microbial gas. On the Bernard Plot, the results for the BH03 SA sample plot are directly above the thermogenic field and to the right of the field typical of microbial gas (Figure 13). During thermogenic gas migration, primarily through sediments with minimal hydrocarbons, heavier alkanes are stripped by various processes, increasing the $C_1/(C_2 + C_3)$ ratio [36,71]. This process typically has little effect on the methane's isotopic composition, as indicated by the vertical arrow in Figure 13. Alternatively, during oxidation of microbial gas, which has a much greater abundance of methane than heavier alkanes, partial oxidation may reduce methane concentrations more rapidly than the scarcity of heavier alkanes, resulting in a decrease in the $C_1/(C_2 + C_3)$ ratio. Oxidation of the methane would also shift the $\delta^{13}C$ (and δD) to more positive values (as indicated by the diagonal arrow in Figure 12).

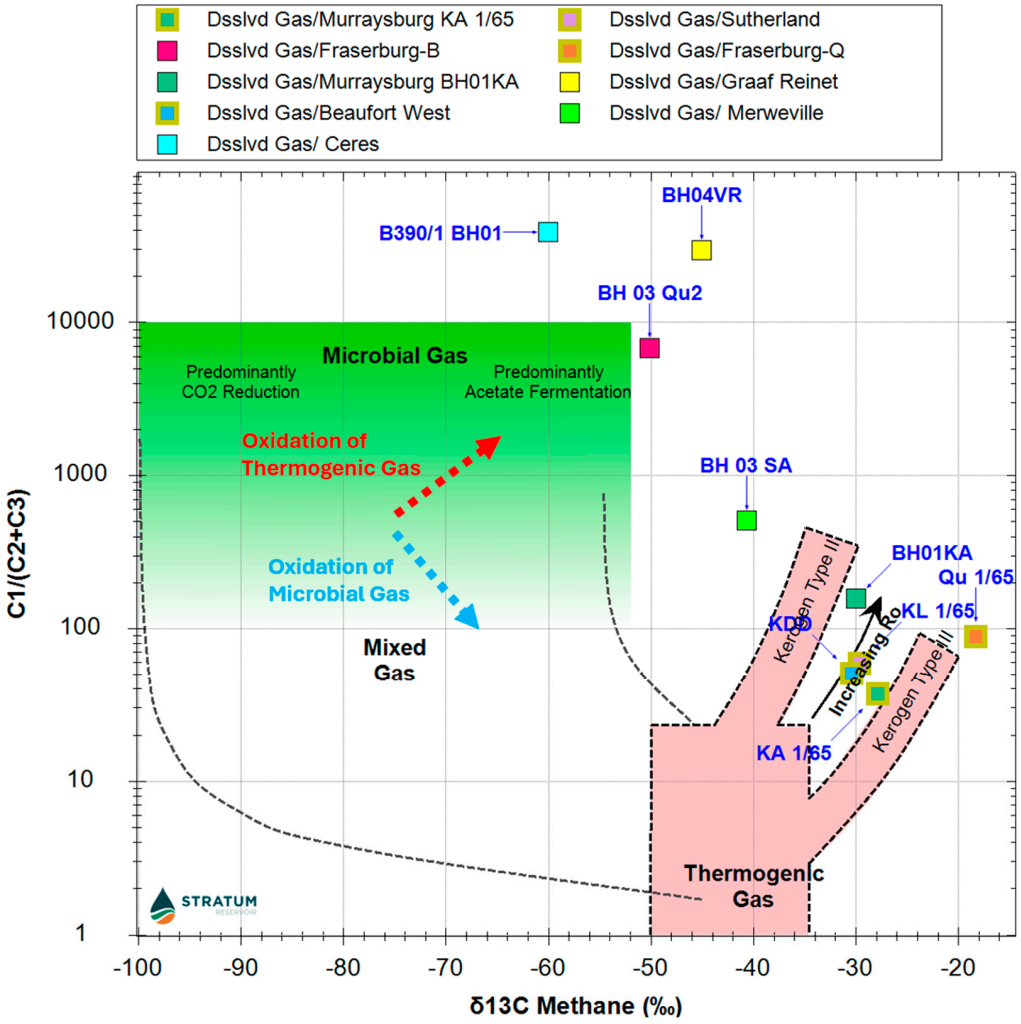


Figure 13. Bernard Plot for the dissolved gas samples from the Ceres, Merweville, Beaufort West, Graaff-Reinet, Murraysburg, Fraserburg-Quaggasfontein, Fraserburg-Beeswater, and Sutherland sites (see legend for symbol colors) (Diagram template based on [70]. The gold outline on datapoints represents samples with isotopic reversals ($\delta^{13}C$ of methane > $\delta^{13}C$ of ethane). The red or blue dashed arrows represent oxidation of a thermogenic gas or microbial gas, respectively.

In Beaufort West, only the KDD legacy well had a sufficiently high dissolved gas concentration for isotopic analysis (Figure 11 and Table 3). The isotopic composition of methane in the dissolved gas sample for the KDD well had a more positive $\delta^{13}C$ value and plots outside the typical range for thermogenic gas (Figure 12). The $\delta^{13}C$ and δD values for the methane for KDD suggest it may be related to geothermal/hydrothermal processes. Considering the history of dolerite intrusions into Karoo Supergroup rock units (the Dwyka, Ecca, Beaufort, and Stormberg groups), it would not be surprising if, with elevated temperatures due to the magmatic intrusions, geothermal gases in the Karoo Basin were produced. The data from KDD well and other data from two published studies on geothermal gas in Germany and Italy were plotted in Figure 14 demonstrating similar isotopic reversals (blue stars and orange asterisks [57,58]. It could be argued that the isotopic composition of the KDD methane results from the oxidation of microbial gas that infiltrated the well. However, the Bernard Plot for the $\delta^{13}C$ and $C_1/(C_2 + C_3)$ results indicates that the KDD dissolved gas sample fits expectations for a relatively mature thermogenic gas (Figure 13). The $\delta^{13}C$ of the ethane in the KDD dissolved gas sample was −36.7 ‰, which, although typical of thermogenic gas, is actually more negative than the $\delta^{13}C$ measured for the methane (−30.39 ‰) in the KDD sample (Figure 14). These isotopic compositions are reversed relative to those usually observed for thermogenic gases. Typically, the lighter alkanes, such as methane, will have more negative $\delta^{13}C$ values than the heavier alkanes, such as ethane [59,72].

In Graaff-Reinet, only the BH04VR groundwater borehole had sufficient hydrocarbon concentrations for isotopic analysis (Figure 11 and Table 3). The isotopic composition of BH04VR suggests the gas is thermogenic in origin (Figure 12). The BH04VR sample had a $C_1/(C_2 + C_3)$ ratio of about 29,300, much greater than normally expected for a thermogenic gas (thermogenic gas typically has a value less than 50 for the $C_1/(C_2 + C_3)$ ratio) and more in line with that expected for a microbial gas [68] (Figure 13). Considering the $\delta^{13}C$ and δD results, the BH04VR sample can be said to lie in the middle of the range of values typically observed for thermogenic gas. The dissolved gas observed in the BH04VR sample likely originated from a thermogenic source. The heavier alkanes are often stripped off during the migration of thermogenic gas through shallower groundwater in non-hydrocarbon-bearing units [70,73,74].

In Murraysburg, Well KA 1/65 and borehole BH01KA had a high enough dissolved gas concentration for isotopic analysis (Figure 11 and Table 3). The isotopic compositions of the dissolved methane from the KA 1/65 well and the BH01KA borehole sample had relatively positive $\delta^{13}C$ values. They plotted to the right of the typical range for thermogenic gas (Figure 12). It is also possible that the isotopic compositions of the KA 1/65 and BH01KA dissolved methane could be interpreted to be very-oxidized microbial gas. However, when examining the Bernard Plot, the $\delta^{13}C$ and $C_1/(C_2 + C_3)$ results indicate that the KA 1/65 and BH01KA dissolved gas samples fit expectations for a relatively mature thermogenic gas (Figure 13). The $\delta^{13}C$ of the ethane in the KA 1/65 dissolved gas sample was −35.1‰, typical of thermogenic gas but more negative than the $\delta^{13}C$ measured for the methane (−27.85‰). This is similar to what was observed for the dissolved gas sample from the deep KDD sample (Figure 14). Again, these isotopic compositions are reversed relative to those usually observed for thermogenic gases. The data from KA 1/65, KDD and other data from two published studies on geothermal gas in Germany and Italy were plotted in Figure 14 demonstrating similar isotopic reversals (blue stars and orange asterisks [57,58]. The $\delta^{13}C$ of the methane and ethane reversal observed in the dissolved gas samples from KDD and KA 1/65 was not observed in the dissolved gas sample collected from BH01KA. This is most likely due to a mixing of a different thermogenic source with the hydrocarbon gas source observed in the KA 1/65 and KDD wells.

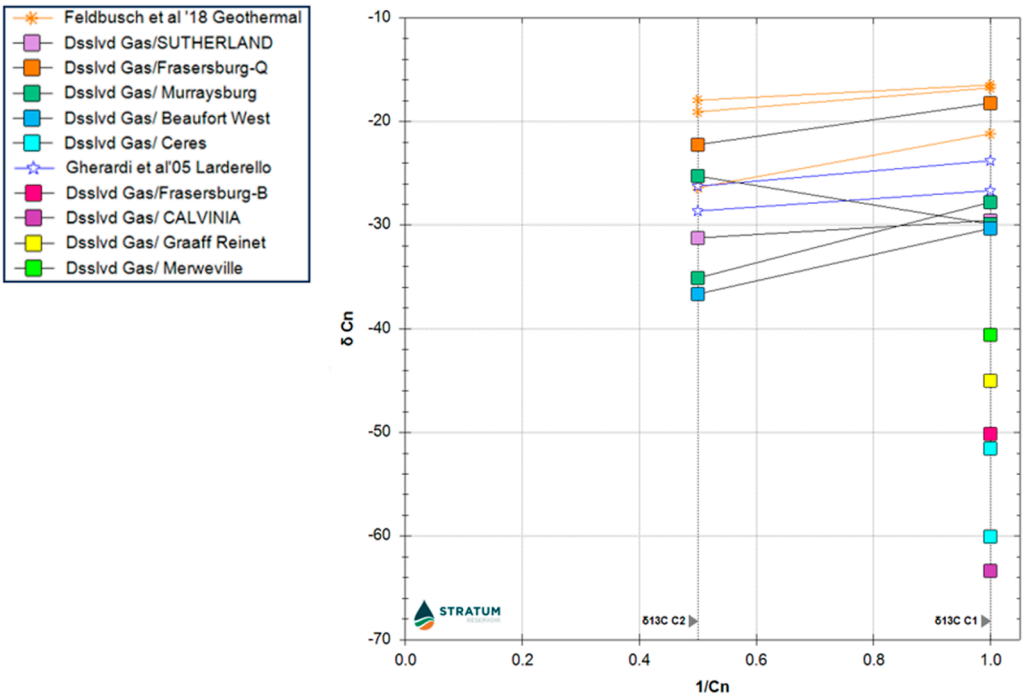


Figure 14. Chung plot showing $\delta^{13}C$ of methane and ethane for dissolved gases from the study area and data from two published studies on geothermal gas in Germany and Italy for which similar isotopic reversals were observed (blue stars and orange asterisks [57,58,75].

In Calvinia, only one groundwater borehole had a sufficient dissolved hydrocarbon concentration for isotopic analysis (Figure 11 and Table 3). The dissolved methane concentration in BH01KC was sufficient for $\delta^{13}C$ analysis but not for δD analysis. The $\delta^{13}C$ of dissolved methane for BH01KC suggests that the gas is primarily microbial (indicated by the black dotted vertical line in Figure 12). This is consistent with the absence of heavier alkanes in the BH01KC dissolved gas sample.

In Fraserburg-Q (Quaggasfontein farm), only well QU 1/65 had a high enough dissolved gas concentration for isotopic analysis (Figure 11 and Table 3). As observed with other deep-basin well samples, the isotopic composition of the dissolved methane for the QU 1/65 sample had a more positive $\delta^{13}C$ of methane values and plotted to the right for the expected values for thermogenic gas (having a more positive $\delta^{13}C$ of methane values) on a diagram of δD vs. $\delta^{13}C$ of methane (Figure 12). Examining the Bernard Plot for the $\delta^{13}C$ of methane and $C_1/(C_2 + C_3)$ results indicates that the QU 1/65 dissolved gas sample fits expectations for a relatively mature thermogenic gas (Figure 13). The $\delta^{13}C$ of the ethane in the QU 1/65 dissolved gas sample was −22.3 ‰, typical of thermogenic gas but more negative than the $\delta^{13}C$ measured for the methane (−18.27 ‰). This is similar to what was observed for the dissolved gas samples from the deep wells KDD and KA 1/65. As discussed previously, these isotopic compositions are reversed relative to those observed for most thermogenic gases. An examination of the $\delta^{13}C$ values for methane and ethane, in the QU 1/65 gas sample also showed an isotopic reversal (Figure 14). The data from KA 1/65, QU 1/64, KDD wells and other data from two published studies on geothermal gas in Germany and Italy were plotted in Figure 14 demonstrating similar isotopic reversals (blue stars and orange asterisks [57,58]).

In Fraserburg-B (Beeswater farm), only the BH03QU2 groundwater borehole had a high enough dissolved gas concentration for isotopic analysis (Figure 11 and Table 3). The isotopic composition of the methane for the BH03QU2 dissolved gas sample had a $\delta^{13}C$ value of −50.14 ‰ and a very negative δD value (−334 ‰), characteristic of microbial gas produced predominantly via the acetate-fermentation-type methanogenic pathway

(Figure 12). When examining the data using a Bernard Plot of $\delta^{13}C$ for methane and $C_1/(C_2 + C_3)$, the BH03QU2 sample is more characteristic of microbial gas than of thermogenic gas (Figure 13).

In Sutherland, only KL 1/65 was sampled and had a sufficient dissolved hydrocarbon concentration for isotopic analysis (Figure 11 and Table 3). As observed for the other deep-basin wells, the methane isotopic composition of the dissolved gas from the KL 1/65 well had a relatively positive $\delta^{13}C$ value and plotted to the right of the typical range for thermogenic gas on a $\delta^{13}C$-δD graph (Figure 12). When examining the $C_1/(C_2 + C_3)$ versus $\delta^{13}C$ of methane results, it can be observed that the KL 1/65 dissolved gas sample plots with the other deep-well dissolved gas samples, which showed characteristics of mature thermogenic gases (Figure 13). The $\delta^{13}C$ of the ethane in the KL 1/65 dissolved gas sample was −31.3 ‰, more negative than the $\delta^{13}C$ measured for the methane (−29.60 ‰). This is similar to what was observed for the other dissolved gas samples from the deep-basin wells, which show isotopic compositions that are reversed relative to those of most thermogenic gases. A plot of $\delta^{13}C$ for methane and ethane versus the inverse number of carbon atoms (a Chung Plot) is shown in Figure 14. The data from KL 1/65, KA 1/65, QU 1/64, KDD wells and other data from two published studies on geothermal gas in Germany and Italy were plotted in Figure 14 demonstrating similar isotopic reversals (blue stars and orange asterisks [57,58]).

5.3. Integration of Well Barrier Failure and Geochemical Tracing

Traced dissolved gas on legacy wells and some groundwater boreholes confirmed leakages due to improper construction and abandonment of legacy wells. This confirmation reaffirms the use of modern industry practices [64] and statutory regulations [39,40] to assess abandonment integrity of legacy wells. The integration of these methods compliments each other on assessing abandonment integrity of legacy wells and can be applied elsewhere to solve similar challenges. Modern industry practices and regulations provide a means on how abandoned wells with completion reports can be assessed whereas geochemical tracing can be used to confirm leakage after well abandonment.

6. Discussions

6.1. Observations of Abandonment Integrity Assessment and Their Consequences

During the construction of these wells, numerous fractures were intersected, which accounted for mud losses during drilling and for loss of cement circulation during casing grouting and well plugging. Additionally, CR 1/68 fractures contributed to rock wall caving which did not allow for good seals when setting packers for well flow rate tests. Considering how natural fractures contributed to the geological formation intersected during drilling, these wells' casing, grouting, completion, plugging, and abandonment were not properly executed as per NORSOK D-010/ISO 16530-2 standards guidelines and do not support fracking in future wells in the vicinity. In addition, most of these wells are over 50 years since drilled (Figure 15), and Kang et al. [24]; McMahon et al. [26]; Davies et al. [27] found that wells of this age tend to lose their ability to isolate and contain hydrocarbons as their cement sheath deteriorates and the well casing corrodes. These observations of well barrier failure in this study area are similar to observations made by Zheng et al. [32]; Doble et al. [33]; Hachem & Kang [34]; Ingraffea et al. [35]; Davies et al. [27].

These wells tested positive for hydrocarbons, but in minor occurrences, and were considered uneconomic due to a lack of flow rates in impermeable shale layers. Recently, these bypassed hydrocarbons in tight shales have been produced using horizontal drilling and hydraulic fracturing. Unfortunately, the use of hydraulic fracturing in the vicinity of

these improperly plugged wells poses a significant risk of groundwater contamination as addressed by Osborn et al. [3]. Observations for groundwater contaminations through improperly abandoned wells in other regions near hydraulic fracturing activities were also concluded by Osborn et al. [3]; Arthur. [29]. Suppose hydraulic fracturing occurs around these improperly abandoned wells in the Karoo region, the same stray methane gas contamination may occur. As a result, guidelines to abandon future wells have been developed (PASA internal report) to enforce proper decommissioning and abandonment.

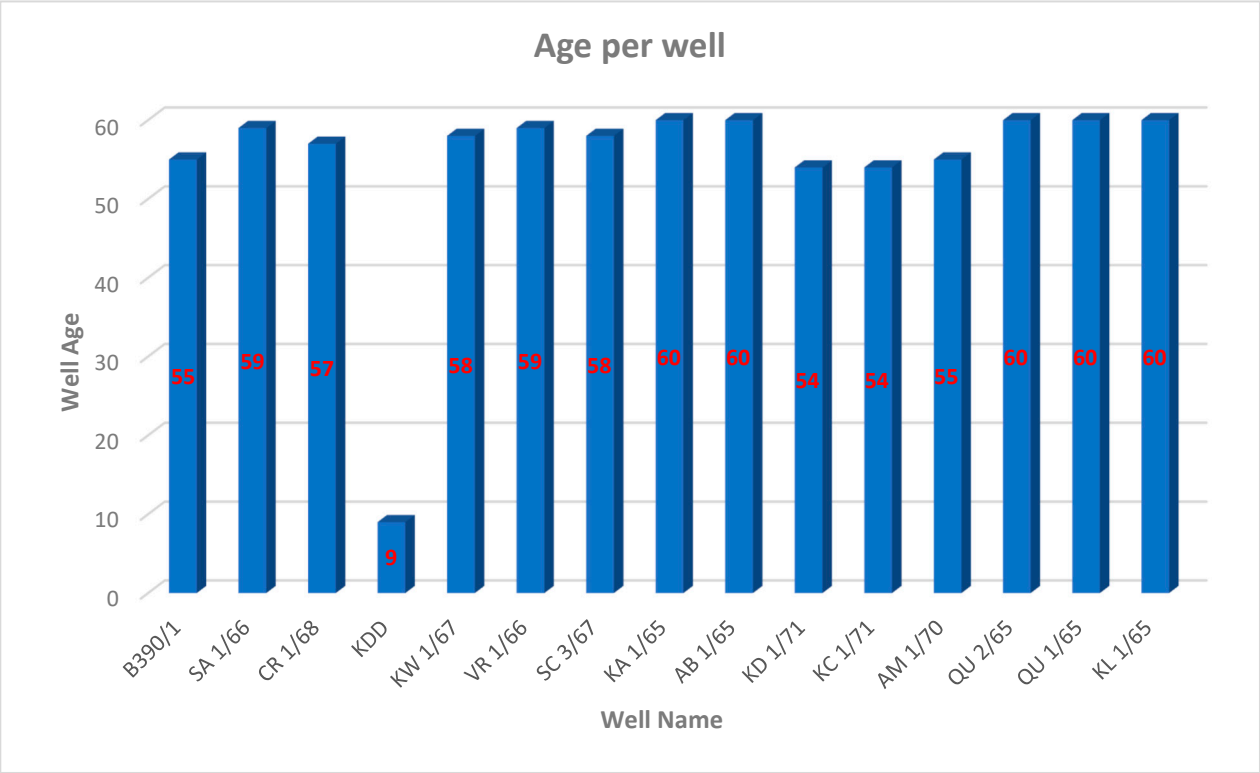


Figure 15. Abandoned well age distribution.

6.2. Dissolved Gas ($\delta^{13}C$ and δD) Isotopic Analysis

The samples from Prince Albert, Aberdeen, Victoria West, Carnarvon, and Williston contained negligible hydrocarbon concentrations. The isotopic compositions of the dissolved gas samples that contained sufficient hydrocarbon concentrations for isotopic analysis showed an extensive range of values, indicating multiple sources of gas in the Karoo Basin, including microbial, thermogenic, and what appears to be geothermal (what could be thermogenic gas that then underwent another phase of heating due to dolerite intrusions). The isotopic results for dissolved methane have been plotted on published diagrams that include ranges of isotopic values expected or observed for gases from geothermal/hydrothermal systems (Figures 15–17). Some of the results suggested microbial gas produced primarily via the CO_2-reduction metabolic pathway, including samples from the Ceres site (B390/1 BH01 and BH02) and the Merweville site (BH03 SA). The isotopic composition of the B390/1 BH02 and BH03SA samples suggested the gas had been subjected to significant oxidation. The BH03SA dissolved gas contained relatively high amounts of ethane compared to the methane detected, suggesting it was a mixture of thermogenic and oxidized microbial gas. One sample from the Fraserburg-Beeswater site, BH03-QU2, was definitely microbial gas (primarily associated with the acetate fermentation metabolic pathway). This observation confirms that the hydrocarbon gas originates from shallow depths and is unrelated to leakage from legacy wells. Another sample, BH04VR from the

Graaff-Reinet site, was typical of thermogenic gas, showing that downhole plugging of VR 1/66 did not maintain its integrity, with the possibility of cross-contamination. However, the rest of the dissolved gas samples, including BH01KA and KA 1/65 (Murraysburg site), KDD (Beaufort West site), QU 1/65 (Fraserburg-Q site), and KL 1/65 (Sutherland site), showed unusually positive $\delta^{13}C$ values, which appear to be characteristic of gases associated with geothermal/hydrothermal sources (Figures 15–17). Given the significant amounts of thermogenic gas detected in these wells, it is evident that the downhole plugs did not maintain their integrity. Dissolved gas in BH01KA showed potential for contamination due to natural fracture pathways, as it is situated 6.5 km from KA 1/65 legacy well. Additionally, isotopic reversals observed in these deep legacy wells have been observed in other basins with geothermal gas sources (Figure 18) [57,58]. Several dissolved gas samples have geothermal signatures, especially those from deep legacy wells in the Karoo Basin. This finding is consistent with the fact that dolerite intrusions have impacted a significant portion of the geologic strata in this region, as depicted in Figure 1 [55,76–78]. Studies of the igneous intrusions in the geologic strata of the Karoo Basin showed significant contact metamorphism on surrounding sediments, with an elevated % of vitrinite reflectance (%Ro) near dolerite sills exceeding 4% Ro [55]. This suggests that the organic matter heated to form thermogenic gas, and that regions of the Karoo Basin with more dolerite intrusions may have experienced an additional heat pulse. The later dolerite intrusions could have allowed isotopically lighter (more negative) methane to migrate out of the system, leaving behind a heavier (more positive) $\delta^{13}C$ of methane values, or the additional dolerite intrusion heating could have cracked other hydrocarbon compounds into methane to form hydrocarbon gas with a more positive $\delta^{13}C$ of methane compared to the $\delta^{13}C$ of ethane.

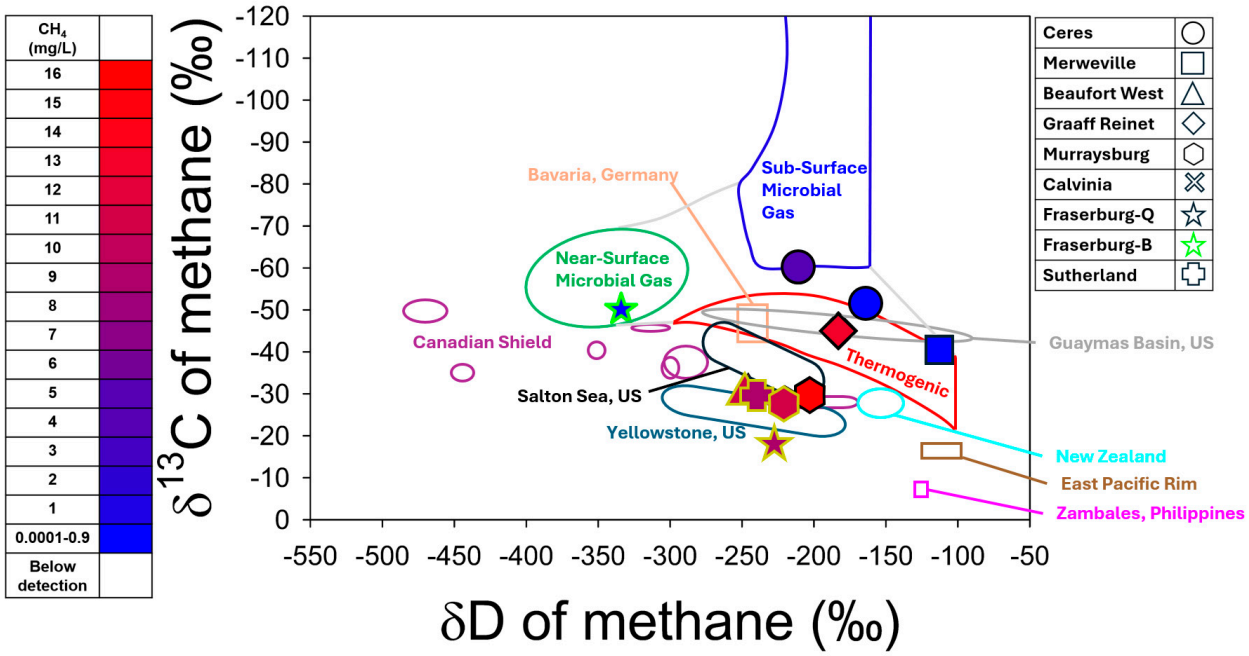


Figure 16. Graph comparing the $\delta^{13}C$ vs. δD of methane domains for methane formed by thermogenic (red outline), near-surface microbial gas (green outline), or subsurface microbial gas (dark blue outline) processes. Also shown are domains for methane from geothermal environments worldwide [75,79–84]. The four datapoints with gold outlines represent samples that exhibit an isotopic reversal ($\delta^{13}C_1 > \delta^{13}C_2$).

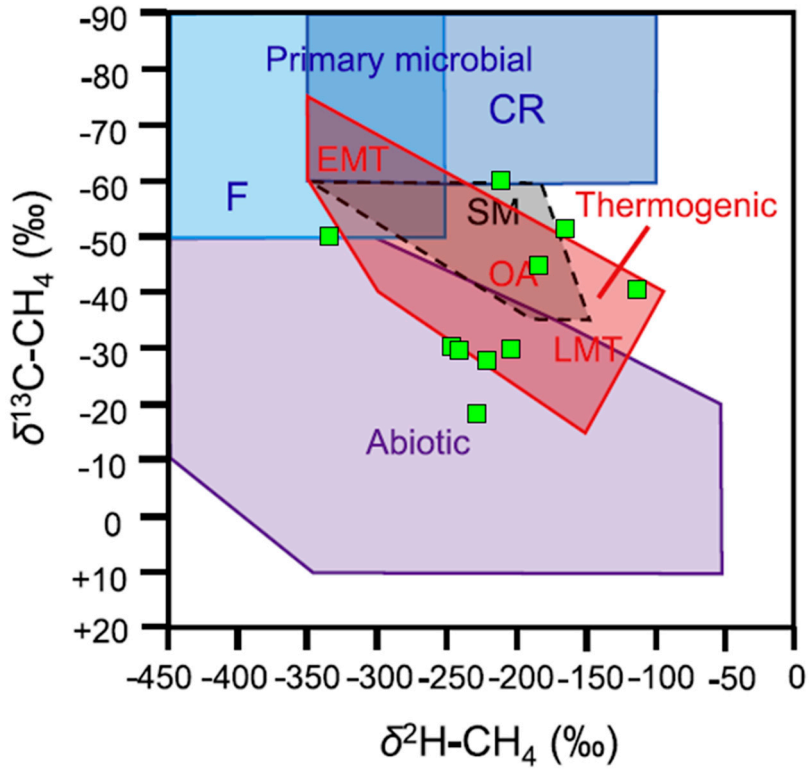


Figure 17. Isotopic results of the dissolved gases (green squares) plotted on a published diagram of the $\delta^{13}C$ versus δD of methane showing compositions associated with different sources of methane including microbial gas formed via methyl-fermentation (F) and CO_2-reduction (CR), early mature thermogenic (EMT) methane, late mature thermogenic (LMT) methane, oil-associated thermogenic (OA) methane, secondary microbial (SM) methane, and methane from geothermal/hydrothermal environments (Abiotic) [85].

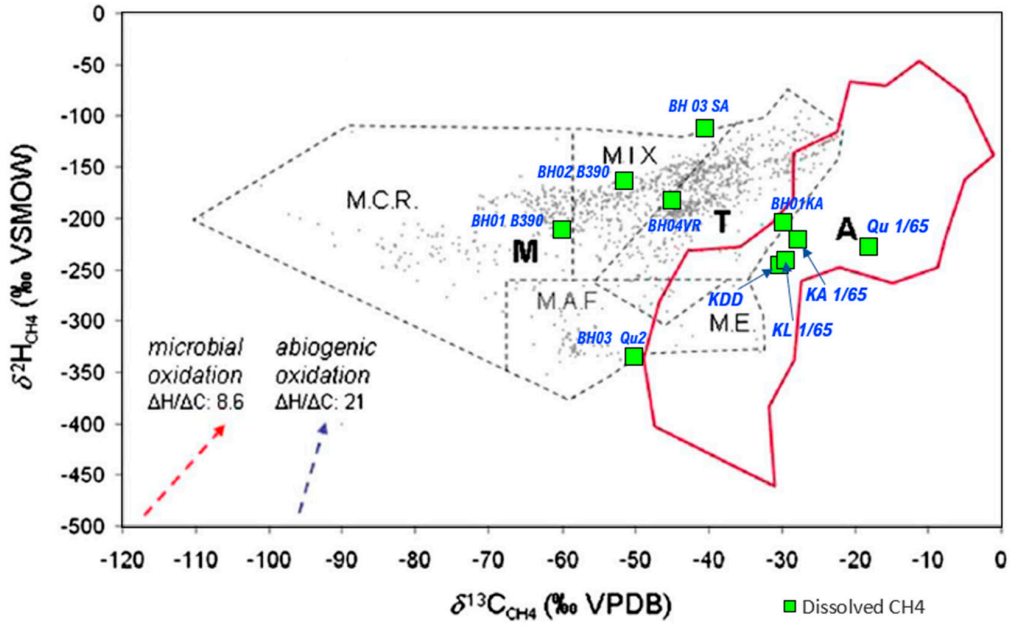


Figure 18. Isotopic results of the dissolved gases (green squares) plotted on a published diagram of the δD vs. $\delta^{13}C$ of methane showing compositions associated with different sources of methane, including microbial gas (M) due to acetate-fermentation via (M.A.F.) or carbonate reduction (M.C.R.), microbial evaporitic (M.E.) [86], thermogenic gas (T), and gas associated with predominantly abiotic (A) processes (outlined in red) [87].

7. Conclusions

This study evaluates abandoned wells in the Karoo Basin by integrating well barrier failure assessment with geochemical tracing analysis. Well barrier failures assessment focused on assessing abandonment integrity using data from well completion reports recorded during operations. The primary objective was to identify well barrier failures and demonstrate potential leaks from the source (Ecca shales) into the receptor (shallow aquifers) using reconstructed well schematics. The key findings presented eleven well barrier failures related to cement integrity between (A) cement and surrounding rock formations (B) casing and surrounding cement; (C) cement plug and casing; (D) cement plug channels; (E) annulus cement channels; (F) fractures in cement between casing and rock formations; (G) casing corrosion; (H) uncased and uncemented sources; (I) an uncemented section above the top of the cement; (J) an unplugged well; and (K) uncemented casing. These leak paths are highly likely to leak from the source to the receptor. To confirm whether leakage and cross-contamination originated from these legacy wells, a geochemical tracing approach was integrated to test for dissolved stray gas in proximal groundwater boreholes. The primary objective was to sample groundwater from legacy wells and shallow boreholes to analyze dissolved gas concentrations and isotopic compositions. Furthermore, we aimed to determine the origin of the gas to assess whether the constituents identified in deep legacy wells have affected shallow aquifers. Based on the samples collected in this study, the areas significantly impacted by hydrocarbon gases are Ceres, Merweville, Fraserburg, Graaff-Reinet, Murraysburg, Beaufort West, and Sutherland. In contrast, Prince Albert, Aberdeen, Victoria West, Carnarvon, and Williston are not impacted. Isotopic geochemical analysis revealed multiple sources of gas, including microbial, thermogenic, and what appears to be geothermal. In Ceres, the results suggest that microbial gas is produced primarily via the CO_2-reduction metabolic pathway. In Merweville, the results indicate a mix of thermogenic and oxidized microbial gas. In Fraserburg-B (Beeswater farm), the results suggest that the gas is primarily microbial, associated with the acetate fermentation metabolic pathway. These observations suggest that the gas originates from shallow depths and is not linked to deep legacy wells. However, the results in the Graaff-Reinet groundwater borehole were typical of thermogenic gas, showing possible contamination driven by leakage from the legacy well within a 1 km radius. The results from BH01KA and KA 1/65 (Murraysburg site), KDD (Beaufort West site), QU 1/65 (Fraserburg-Q site), and KL 1/65 (Sutherland site) showed an unusually positive $\delta^{13}C$ of methane values, which appear to be characteristic of gases associated with geothermal/hydrothermal sources. The leakage pathway at BH01KA may be related to natural fractures (either fault- or dolerite-induced), as it is located 6.5 km from the legacy well. Since a significant amount of thermogenic-type gas was detected in KA 1/65, KDD, QU 1/65, and KL 1/65, it is evident that the downhole plugs did not hold integrity. This observation suggests that hydraulic fracturing near these legacy wells may pose a significant risk of gas leakage. Comparing it with other regions globally, the Karoo Basin possesses similar consequential impact. The outcome of this study encouraged the development of onshore decommissioning guidelines for future wells to prevent continued well leakage after decommissioning and abandonment. This study acknowledges that of fifteen legacy wells investigated, only four wells have been sampled, and the results were inferred to the other eleven wells not sampled, which may present different perspectives. Future innovative solutions can suggest potential differences to the observations presented in this study. In addition, the limitation of aqueous chemistry in assessing the potential impacts of brine and secondary oxidation in shallow aquifers. Future research should focus on water quality assessment due to methane secondary oxidation and the application of using geophysical investigation to interpret subsurface structural complexity and delineate structures that may cause leakage into the shallow aquifer (e.g., faults, dolerite intrusions,

and thermal spring feeders). Such work will help exempt such areas from shale gas extraction activities and improve our understanding of potential environmental problems, whilst encouraging progressive oil and gas development in an environmentally friendly (safe) manner.

Author Contributions: Conceptualization, M.M., T.K. and T.M.; methodology, M.M.; software, M.M., M.T.M. and K.H.; validation, T.K., Y.X., M.T.M. and K.H.; formal analysis, M.M. and L.B.; investigation, M.M., T.M., T.K., M.T.M. and K.H.; resources, T.K., M.T.M. and K.H.; data curation, M.M., L.B. and T.M.; writing—original draft preparation, M.M.; writing—review and editing, M.M., L.B., T.M., T.K., Y.X., M.T.M. and K.H.; visualization, M.M.; supervision, T.K. and Y.X.; project administration, M.M. and T.M.; funding acquisition, M.M. and T.M. All authors have read and agreed to the published version of the manuscript.

Funding: This research was funded by Petroleum Agency SA (PASA).

Data Availability Statement: The raw data supporting the conclusions of this article will be made available by the authors upon request.

Acknowledgments: This project contributes to studies on the environmental impacts of shale gas development in South Africa. Special thanks go to PASA for supporting and providing data to complete this study; Stratum Reservoir for assistance with laboratory analyses; Iyani Nedzamba for ArcGIS (ArcMap 10.6.2) data management; and Norman Baloyi, Phuthi Seanego, and Randall de Wet for field sampling.

Conflicts of Interest: Authors Murendeni Mugivhi and Tshifhiwa Mabidi were employed by the company Petroleum Agency of South Africa. Authors Myles T. Moore and Keith Hackley were employed by the company Stratum Reservoir (Isotech), LLC. Author Lucky Baloyi was employed by the company Department of Water and Sanitation, Belville Office. The remaining authors declare that the research was conducted in the absence of any commercial or financial relationships that could be construed as a potential conflict of interest. The authors declare that this study received funding from Petroleum Agency SA. The funder was not involved in the study design, collection, analysis, interpretation of data, the writing of this article or the decision to submit it for publication.

References

1. Academy of Science of South Africa (ASSAF). *South Africa's Technical Readiness to Support the Shale Gas Industry*; Academy of Science South Africa: Pretoria, South Africa, 2016; ISBN 978-0-9946852-7-8. Available online: https://research.assaf.org.za (accessed on 12 October 2016).
2. Cooper, J.; Stamford, L.; Azapagic, A. Shale Gas: A Review of the Economic, Environmental, and Social Sustainability. *Energy Technol.* **2016**, *4*, 772–792. [CrossRef]
3. Osborn, S.G.; Vengosh, A.; Warner, N.R.; Jackson, R.B. Methane contamination of drinking water accompanying gas-well drilling and hydraulic fracturing. *Environ. Sci.* **2011**, *108*, 8172–8176. [CrossRef] [PubMed]
4. Moore, M.T.; Mugivhi, M.; Hackley, K.C. Baseline assessment of groundwater quality in the Karoo Basin, South Africa. In Proceedings of the 2024 Goldschmidt Conference, Chicago, IL, USA, 18–23 August 2024.
5. Morais, T.A.; Fleming, N.A.; Attalage, D.; Mayer, B.; Mayer, K.U.; Ryan, M.C. Field investigation of the transport and attenuation of fugitive methane in shallow groundwater around an oil and gas well with gas migration. *Sci. Total. Environ.* **2023**, *908*, 168246. [CrossRef] [PubMed]
6. Segal, D.C.; Visser, A.; Bridge, C. Noble Gas Analyses to Distinguish Between Surface and Subsurface Brine Releases at a Legacy Oil Site. *Groundwater* **2024**, *62*, 645–655. [CrossRef]
7. Shaheen, S.W.; Wen, T.; Herman, A.; Brantley, S.L. Geochemical Evidence of Potential Groundwater Contamination with Human Health Risks where Hydraulic Fracturing Overlaps with Extensive Legacy Hydrocarbon Extraction. *Environ. Sci. Technol.* **2022**, *56*, 10010–10019. [CrossRef] [PubMed]
8. Whyte, C.J.; Vengosh, A.; Warner, N.R.; Jackson, R.B.; Muehlenbachs, K.; Schwartz, F.W.; Darrah, T.H. Geochemical evidence for fugitive gas contamination and associated water quality changes in drinking-water wells from Parker County, Texas. *Sci. Total. Environ.* **2021**, *780*, 146555. [CrossRef]
9. Schout, G.; Griffioen, J.; Hassanizadeh, S.M.; de Lichtbuer, G.C.; Hartog, N. Occurrence and fate of methane leakage from cut and buried abandoned gas wells in the Netherlands. *Sci. Total Environ.* **2019**, *659*, 773–782. [CrossRef]

10. Vigneron, A.; Bishop, A.; Alsop, E.B.; Hull, K.; Rhodes, I.; Hendricks, R.; Head, I.M.; Tsesmetzis, N. Microbial and isotopic evidence for methane cycling in hydrocarbon-containing groundwater from the Pennsylvania region. *Front. Microbiol.* **2017**, *8*, 593. [CrossRef]
11. Montcoudiol, N.; Isherwood, C.; Gunning, A.; Kelly, T.; Younger, P.L. Shale gas impacts on groundwater resources: Understanding the behavior of a shallow aquifer around a fracking site in Poland. *Energy Procedia* **2017**, *125*, 106–115. [CrossRef]
12. LeDoux, S.T.M.; Szynkiewicz, A.; Faiia, A.M.; Mayes, M.A.; McKinney, M.L.; Dean, W.G. Chemical and isotope compositions of shallow groundwater in areas impacted by hydraulic fracturing and surface mining in the Central Appalachian Basin, Eastern United States. *Appl. Geochem.* **2016**, *71*, 73–85. [CrossRef]
13. Brantley, H.L.; Thoma, E.D.; Squier, W.C.; Guven, B.B.; Lyon, D. Assessment of methane emissions from oil and gas production pads using mobile measurements. *Environ. Sci. Technol.* **2014**, *48*, 14508–14515. [CrossRef] [PubMed]
14. Baldassare, F.J.; McCaffrey, M.A.; Harper, J.A. A geochemical context for stray gas investigations in the northern Appalachian Basin: Implications of analyses of natural gases from Neogene-through Devonian-age strata. *Am. Assoc. Pet. Geol. Bull.* **2014**, *98*, 341–372. [CrossRef]
15. Molofsky, L.J.; Connor, J.A.; Van De Ven, C.J.; Hemingway, M.P.; Richardson, S.D.; Strasert, B.A.; McGuire, T.M.; Paquette, S.M. A review of physical, chemical, and hydrogeologic characteristics of stray gas migration: Implications for investigation and remediation. *Sci. Total. Environ.* **2021**, *779*, 146234. [CrossRef]
16. Jackson, R.E.; Gorody, A.W.; Mayer, B.; Roy, J.W.; Ryan, M.C.; Van Stempvoort, D.R. Groundwater protection and unconventional gas extraction: The critical need for field-based hydrogeological research. *Groundwater* **2013**, *51*, 488–510. [CrossRef]
17. Hohne, D.; de Lange, F.; Esterhuyse, S.; Lollar, B.S. Case study: Methane gas in a groundwater system located in a dolerite ring structure in the Karoo Basin; South Africa. *South Afr. J. Geol.* **2019**, *122*, 357–368. [CrossRef]
18. Stroebel, D.H.; Thiart, C.; De Wit, M. Towards defining a baseline status of scarce groundwater resources in anticipation of hydraulic fracturing in the eastern cape karoo, South Africa: Salinity, aquifer yields and groundwater levels. In *Geological Society Special Publication*; Geological Society of London: London, UK, 2019; Volume 479, pp. 129–145. [CrossRef]
19. Harkness, J.S.; Swana, K.; Eymold, W.K.; Miller, J.; Murray, R.; Talma, S.; Whyte, C.J.; Moore, M.T.; Maletic, E.L.; Vengosh, A.; et al. Pre-drill Groundwater Geochemistry in the Karoo Basin, South Africa. *Groundwater* **2018**, *56*, 187–203. [CrossRef] [PubMed]
20. Eymold, W.K.; Swana, K.; Moore, M.T.; Whyte, C.J.; Harkness, J.S.; Talma, S.; Murray, R.; Moortgat, J.B.; Miller, J.; Vengosh, A.; et al. Hydrocarbon-Rich Groundwater above Shale-Gas Formations: A Karoo Basin Case Study. *Groundwater* **2018**, *56*, 204–224. [CrossRef]
21. Miller, J.; Swana, K.; Talma, S.; Vengosh, A.; Tredoux, G.; Murray, R.; Butler, M. O, H, CDIC, Sr, B and 14C Isotope Fingerprinting of Deep Groundwaters in the Karoo Basin, South Africa as a Precursor to Shale Gas Exploration. *Procedia Earth Planet. Sci.* **2015**, *13*, 211–214. [CrossRef]
22. Talma, A.S.; Esterhuyse, C. Isotopic clues to the origin of methane emissions in the Karoo. *South Afr. J. Geol.* **2015**, *118*, 45–54. [CrossRef]
23. Kiran, R.; Teodoriu, C.; Dadmohammadi, Y.; Nygaard, R.; Wood, D.; Mokhtari, M.; Salehi, S. Identification and evaluation of well integrity and causes of failure of well integrity barriers (A review). *J. Nat. Gas Sci. Eng.* **2017**, *45*, 511–526. [CrossRef]
24. Kang, M.; Brandt, A.R.; Zheng, Z.; Boutot, J.; Yung, C.; Peltz, A.S.; Jackson, R.B. Orphaned oil and gas well stimulus-maximizing economic and environmental benefits. *Elementa* **2021**, *9*, 161. [CrossRef]
25. Gianoutsos, N.J.; Haase, K.B.; Birdwell, J.E. Geologic sources and well integrity impact methane emissions from orphaned and abandoned oil and gas wells. *Sci. Total. Environ.* **2024**, *912*, 169584. [CrossRef] [PubMed]
26. McMahon, P.B.; Thomas, J.C.; Crawford, J.T.; Dornblaser, M.M.; Hunt, A.G. Methane in groundwater from a leaking gas well, Piceance Basin, Colorado, USA. *Sci. Total Environ.* **2018**, *634*, 791–801. [CrossRef]
27. Davies, R.J.; Almond, S.; Ward, R.S.; Jackson, R.B.; Adams, C.; Worrall, F.; Herringshaw, L.G.; Gluyas, J.G.; Whitehead, M.A. Oil and gas wells and their integrity: Implications for shale and unconventional resource exploitation. *Mar. Pet. Geol.* **2014**, *56*, 239–254. [CrossRef]
28. Kang, M.; Boutot, J.; McVay, R.C.; A Roberts, K.; Jasechko, S.; Perrone, D.; Wen, T.; Lackey, G.; Raimi, D.; Digiulio, D.C.; et al. Environmental risks and opportunities of orphaned oil and gas wells in the United States. *Environ. Res. Lett.* **2023**, *18*, 074012. [CrossRef]
29. Arthur, J.D. Gas Well Integrity and Associated Gas Migration Investigations in the Marcellus Shale. *J. Natl. Acad. Forensic Eng.* **2016**, *33*, 1–13. [CrossRef]
30. Zhai, L.; Xun, Y.; Liu, H.; Qi, B.; Wu, J.; Wang, Y.; Chen, C. An investigation of hydraulic fracturing initiation and location of hydraulic fracture in preforated oil shale formations. *Sci. Rep.* **2025**, *15*, 4196. [CrossRef]
31. McCaffrey, M.A.; Kornacki, A.S.; Laughrey, C.D.; Patterson, B.A. Stray gas source determination using forensic geochemical data. *Interpretation* **2023**, *11*, SC11–SC26. [CrossRef]

32. Zheng, D.; Turhan, C.; Wang, N.; Wu, C.; Ashok, P.; Van Oort, E. Prioritizing Wells for Repurposing or Permanent Abandonment Based on Generalized Well Integrity Risk Analysis. Available online: https://ssrn.com/abstract=5001633 (accessed on 16 December 2025). [CrossRef]
33. Doble, R.; Mallants, D.; Huddlestone-Holmes, C.; Peeters, L.J.; Kear, J.; Turnadge, C.; Wu, B.; Noorduijn, S.; Arjomand, E. A multi-stage screening approach to evaluate risks from inter-aquifer leakage associated with gas well and water bore integrity failure. *J. Hydrol.* **2023**, *618*, 129244. [CrossRef]
34. El Hachem, K.; Kang, M. Reducing oil and gas well leakage: A review of leakage drivers, methane detection and repair options. *Environ. Res. Infrastruct. Sustain.* **2023**, *3*, 012002. [CrossRef]
35. Ingraffe, A.R.; Wells, M.T.; Santoro, R.L.; Shonkoff, S.B.C. Assessment and risk analysis of casing and cement impairment in oil and gas wells in Pennsylvania, 2000–2012. *Proc. Natl. Acad. Sci. USA* **2014**, *111*, 10955–10960. [CrossRef] [PubMed]
36. Kreuzer, R.L.; Darrah, T.H.; Grove, B.S.; Moore, M.T.; Warner, N.R.; Eymold, W.K.; Whyte, C.J.; Mitra, G.; Jackson, R.B.; Vengosh, A.; et al. Structural and Hydrogeological Controls on Hydrocarbon and Brine Migration into Drinking Water Aquifers in Southern New York. *Groundwater* **2018**, *56*, 225–244. [CrossRef]
37. Harkness, J.; Darrah, T.H.; Warner, N.R.; Whyte, C.J.; Moore, M.T.; Millot, R.; Kloppmann, W.; Jackson, R.B.; Vengosh, A. The geochemistry of naturally occurring methane and saline groundwater in an area of unconventional shale gas development. *Geochim. Cosmochim. Acta* **2017**, *208*, 302–334. [CrossRef]
38. Khalifeh, M.; Saasen, A. *Introduction to Permanent Plug and Abandonment of Wells*; Ocean Engineering & Oceanography, Vol. 12; Springer International Publishing: Cham, Switzerland, 2020. [CrossRef]
39. Oil and Gas UK. *Guidelines for Suspension and Abandonment of Wells*; Oil and Gas UK: Aberdeen, UK, 2018.
40. *NORSOK Standard D.-010*; Well Integrity in Drilling and Well Operations. Standard Norge: Oslo, Norway, 2013. Available online: www.standard.no/petroleum (accessed on 12 October 2016).
41. Gulliford, A.R.; Flint, S.S.; Hodgson, D.M. Crevasse splay processes and deposits in an ancient distributive fluvial system: The lower Beaufort Group, South Africa. *Sediment. Geol.* **2017**, *358*, 1–18. [CrossRef]
42. Tankard, A.; Welsink, H.; Aukes, P.; Newton, R.; Stettler, E. Tectonic evolution of the Cape and Karoo basins of South Africa. *Mar. Pet. Geol.* **2009**, *26*, 1379–1412. [CrossRef]
43. Corner, B.; Durrheim, R.J. An Integrated Geophysical and Geological Interpretation of the Southern African Lithosphere. In *Geology of Southwest Gondwana*; Springer: Cham, Switzerland, 2018; pp. 19–61. [CrossRef]
44. Mckay, M.P. Integrated Geochronology and Petrogenesis of Volcanic Suites for Integrated Geochronology and Petrogenesis of Volcanic Suites for Tectonic Sedimentary Studies: Karoo Basin, South Africa. 2015. [Online]. Available online: https://researchrepository.wvu.edu/etd (accessed on 12 October 2016).
45. López-Gamundí, O. Permian plate margin volcanism and tuffs in adjacent basins of west Gondwana: Age constraints and common characteristics. *J. South Am. Earth Sci.* **2006**, *22*, 227–238. [CrossRef]
46. Woodford, A.C.; Chevallier, L. *Hydrogeology of the Karoo Basin: Current Knowledge and Future Needs, Pretoria*; Water Research Commission: Pretoria, South Africa, 2002.
47. Visser, J.N.J.; Van Niekerk, B.N.; Van Der Merwe, S.W. Sediment transport of the Late Palaeozoic glacial Dwyka Group in the southwestern Karoo Basin. *South Afr. J. Geol.* **1997**, *100*, 223–236.
48. Schulz, H.-M.; Chere, N.; Geel, C.; Booth, P.; de Wit, M.J. Is the Postglacial History of the Baltic Sea an Appropriate Analogue for the Formation of Black Shales in the Lower Ecca Group (Early Permian) of the Karoo Basin, South Africa? In *Origin and Evolution of the Cape Mountains and Karoo Basin*; Springer: Cham, Switzerland, 2016; pp. 111–117. [CrossRef]
49. De Kock, M.O.; Beukes, N.J.; Adeniyi, E.O.; Cole, D.; Götz, A.E.; Geel, C.; Ossa, F.-G. Deflating the shale gas potential of South Africa's Main Karoo basin. *South Afr. J. Sci.* **2017**, *113*, 12. [CrossRef]
50. Chukwuma, K.; Tsikos, H.; Horsfield, B.; Schulz, H.M.; Harris, N.B.; Frazenburg, M. The effects of Jurassic igneous intrusions on the generation and retention of gas shale in the Lower Permian source-reservoir shales of Karoo Basin, South Africa. *Int. J. Coal Geol.* **2023**, *269*, 104219. [CrossRef]
51. Nolte, S.; Geel, C.; Amann-Hildenbrand, A.; Krooss, B.M.; Littke, R. Petrophysical and geochemical characterization of potential unconventional gas shale reservoirs in the southern Karoo Basin, South Africa. *Int. J. Coal Geol.* **2019**, *212*, 103249. [CrossRef]
52. Nengovhela, V.; Linol, B.; Bezuidenhout, L.; Dhansay, T.; Muedi, T.; de Wit, M.J. Shale gas leakage in lower ecca shales during contact metamorphism by dolerite sill intrusions in the Karoo basin, South Africa. *South Afr. J. Geol.* **2021**, *124*, 443–464. [CrossRef]
53. Johnson, M.R.; Van Vuuren, C.J.; Hegenberger, W.F.; Key, R.; Show, U. Stratigraphy of the Karoo Supergroup in southern Africa: An overview. *J. Afr. Earth Sci.* **1996**, *23*, 3–15. [CrossRef]
54. de Vargas, M.R.; da Silveira, A.S.; Bressane, A.; D'Avila, R.S.F.; Faccion, J.E.; Paim, P.S.G. The Devonian of the Paraná Basin, Brazil: Sequence stratigraphy, paleogeography, and SW Gondwana interregional correlations. *Sediment. Geol.* **2020**, *408*, 105768. [CrossRef]
55. Aarnes, I.; Svensen, H.; Polteau, S.; Planke, S. Contact metamorphic devolatilization of shales in the Karoo Basin, South Africa, and the effects of multiple sill intrusions. *Chem. Geol.* **2011**, *281*, 181–194. [CrossRef]

56. Smithard, T.; Bordy, E.M.; Reid, D. The effect of dolerite intrusions on the hydrocarbon potential of the Lower Permian Whitehill Formation (Karoo Supergroup) in South Africa and southern Namibia: A preliminary study. *South Afr. J. Geol.* **2015**, *118*, 489–510. [CrossRef]
57. Gherardi, F.; Panichi, C.; Gonfiantini, R.; Magro, G.; Scandiffio, G. Isotope systematics of C-bearing gas compounds in the geothermal fluids of Larderello, Italy. *Geothermics* **2005**, *34*, 442–470. [CrossRef]
58. Feldbusch, E.; Wiersberg, T.; Zimmer, M.; Regenspurg, S. Origin of gases from the geothermal reservoir Groß Schönebeck (North German Basin). *Geothermics* **2018**, *71*, 357–368. [CrossRef]
59. Laughrey, C.D. Produced Gas and Condensate Geochemistry of the Marcellus Formation in the Appalachian Basin: Insights into Petroleum Maturity, Migration, and Alteration in an Unconventional Shale Reservoir. *Minerals* **2022**, *12*, 1222. [CrossRef]
60. Fourie, F.; Allwright, A.; Esterhuyse, S.; Govender, N.; Makiwane, N. *Characterisation and Protection of Potential Deep Aquifers in South Africa*; Water Research Commission: Pretoria, South Africa, 2020; WRC Report 2434/1: 19; Available online: www.wrc.org.za (accessed on 12 October 2016).
61. Mahed, G. Development of a conceptual geohydrological model for a fractured rock aquifer in the Karoo, near Sutherland, South Africa. *South Afr. J. Geol.* **2016**, *119*, 33–38. [CrossRef]
62. Adams, S.; Titus, R.; Pietersen, K.; Tredoux, G.; Harris, C. Hydrochemical characteristics of aquifers near Sutherland in the Western Karoo, South Africa. *J. Hydrol.* **2001**, *241*, 91–103. [CrossRef]
63. Senger, K.; Buckley, S.J.; Chevallier, L.; Fagereng, Å.; Galland, O.; Kurz, T.H.; Ogata, K.; Planke, S.; Tveranger, J. Fracturing of doleritic intrusions and associated contact zones: Implications for fluid flow in volcanic basins. *J. Afr. Earth Sci.* **2015**, *102*, 70–85. [CrossRef]
64. *ISO 16530-2:2017*; N.N. (ISO), Petroleum and Natural Gas Industries—Well Integrity Part 2: Well Integrity for the Operational Phase. CEN-CENELEC Management Centre: Bruxelles, Brussels, 2017.
65. Wu, B.; Doble, R.; Turnadge, C.; Mallants, D. Well failure mechanisms and conceptualisation of reservoir-aquifer failure pathways. In Proceedings of the Society of Petroleum Engineers—SPE Asia Pacific Oil and Gas Conference and Exhibition, Perth, Australia, 25–27 October 2016. [CrossRef]
66. Tveit, M.R.; Khalifeh, M.; Nordam, T.; Saasen, A. The fate of hydrocarbon leaks from plugged and abandoned wells by means of natural seepages. *J. Pet. Sci. Eng.* **2021**, *196*, 108004. [CrossRef]
67. Coleman, D.D.; Liu, C.-L.; Hackley, K.C.; Pelphrey, S.R. Isotopic Identification of Landfill Methane. 1995. Available online: https://archives.datapages.com/data/deg/1995/002002/95_deg020095.htm (accessed on 16 December 2025).
68. Taylor, S.W.; Lollar, B.S.; Wassenaar, L.I. Bacteriogenic ethane in near-surface aquifers: Implications for leaking hydrocarbon well bores. *Environ. Sci. Technol.* **2000**, *34*, 4727–4732. [CrossRef]
69. Claypool, G.E.; Kvenvolden, K.A. Methane and other hydrocarbon gases in marine sediment. *Annu. Rev. Earth Planet. Sci.* **1983**, *11*, 299–327. [CrossRef]
70. Bernard, B.B.; Brooks, J.M.; Sackett, W.M. Natural gas seepage in the Gulf of Mexico. *Earth Planet. Sci. Lett.* **1976**, *31*, 48–54. [CrossRef]
71. Moore, M.T.; Vinson, D.S.; Whyte, C.J.; Eymold, W.K.; Walsh, T.B.; Darrah, T.H. Differentiating between biogenic and thermogenic sources of natural gas in coalbed methane reservoirs from the Illinois Basin using noble gas and hydrocarbon geochemistry. *Geol. Soc. Spec. Publ.* **2018**, *468*, 151–188. [CrossRef]
72. Burruss, R.C.; Laughrey, C.D. Carbon and hydrogen isotopic reversals in deep basin gas: Evidence for limits to the stability of hydrocarbons. *Org. Geochem.* **2010**, *41*, 1285–1296. [CrossRef]
73. Coleman, D.D.; Meents, W.F.; Liu, C.-L.; Keogh, R.A. *Isotopic Identification of Leakage Gas from Underground Storage Reservoirs—A Progress Report*; Illinois Petroleum Series 111; Illinois State Geological Survey: Champaign, IL, USA, 1977; pp. 1–10.
74. Whiticar, M.J. A geochemical perspective of natural gas and atmospheric methane. *Org. Geochem.* **1990**, *16*, 531–547. [CrossRef]
75. Chung, H.M.; Gormly, J.R.; Squires, R.M. "Origin of gaseous hydrocarbons in subsurface environments" theoretical considerations of carbon isotope distribution. *Chem. Geol.* **1988**, *71*, 97–104. [CrossRef]
76. Campbell, R.D. Identifying Methane Emissions with Isotopic and Hydrochemical Clues to Their Origin Across Selected Areas of the Karoo Basin, South Africa. Master's Thesis, Nelson Mandela University, Gqeberha, South Africa.
77. Linol, B.; Chere, N.; Muedi, T.; Nengovhela, V.; de Wit, M.J. Deep Borehole Lithostratigraphy and Basin Structure of the Southern Karoo Basin Re-Visited. In *Origin and Evolution of the Cape Mountains and Karoo Basin*; Springer: Cham, Switzerland, 2016; pp. 3–16. [CrossRef]
78. Chere, N.; Linol, B.; de Wit, M.; Schulz, H.M. Lateral and temporal variations of black shales across the southern karoo basin—Implications for shale gas exploration. *South Afr. J. Geol.* **2017**, *120*, 541–564. [CrossRef]
79. Sherwood, B.; Fritz, P.; Frape, S.K.; Macko, S.A.; Weise, S.M.; Welhan, J.A. Methane occurrences in the Canadian Shield. *Chem. Geol.* **1988**, *71*, 223–236. [CrossRef]
80. Welhan, J.A. Origins of methane in hydrothermal systems. *Chem. Geol.* **1988**, *71*, 183–198. [CrossRef]

81. Möller, P.; Weise, S.M.; Althaus, E.; Bach, W.; Behr, H.J.; Borchardt, R.; Bräuer, K.; Drescher, J.; Erzinger, J.; Faber, E.; et al. Paleofluids and recent fluids in the upper continental crust: Results from the German Continental Deep Drilling Program (KTB). *J. Geophys. Res. Solid Earth* **1997**, *102*, 18233–18254. [CrossRef]
82. Welhan, J.A.; Lupton, J.E. Light Hydrocarbon Gases in Guaymas Basin Hydrothermal Fluids: Thermogenic Versus Abiogenic Origin. *AAPG Bull.* **1987**, *71*, 215–223. [CrossRef]
83. Lyon, G.L.; Hulston, J.R. Carbon and hydrogen isotopic compositions of New Zealand geothermal gases. *Geochim. Cosmochim. Acta* **1984**, *48*, 1161–1171. [CrossRef]
84. Abrajano, T.A.; Sturchio, N.C.; Bohlke, J.K.; Lyon, G.L.; Poreda, R.J.; Stevens, C.M. Methane-hydrogen gas seeps, Zambales Ophiolite, Philippines: Deep or shallow origin? *Chem. Geol.* **1988**, *71*, 211–222. [CrossRef]
85. Milkov, A.V.; Faiz, M.; Etiope, G. Geochemistry of shale gases from around the world: Composition, origins, isotope reversals and rollovers, and implications for the exploration of shale plays. *Org. Geochem.* **2020**, *143*, 103997. [CrossRef]
86. Tazaz, A.M.; Bebout, B.M.; Kelley, C.A.; Poole, J.; Chanton, J.P. Redefining the isotopic boundaries of biogenic methane: Methane from endoevaporites. *Icarus* **2013**, *224*, 268–275. [CrossRef]
87. Etiope, G.; Lollar, B.S. Abiotic methane on earth. *Rev. Geophys.* **2013**, *51*, 276–299. [CrossRef]

Disclaimer/Publisher's Note: The statements, opinions and data contained in all publications are solely those of the individual author(s) and contributor(s) and not of MDPI and/or the editor(s). MDPI and/or the editor(s) disclaim responsibility for any injury to people or property resulting from any ideas, methods, instructions or products referred to in the content.